Digital Microfluidic (DMF) devices based on electrowetting on dielectric (EWOD) for biological applications

Ms. Kshirsagar Saniya Sanjay

A Thesis Submitted to
Indian Institute of Technology Hyderabad
In Partial Fulfillment of the Requirements for
The Degree of Master of Technology

Department of Biomedical Engineering

June 2018

Approval Sheet

This Thesis entitled Digital Microfluidic (DMF) devices based on electrowetting on dielectric (EWOD) for biological applications by Ms. Kshirsagar Saniya Sanjay is approved for the degree of Master of Technology from IIT Hyderabad

Dr. Lopamudra Giri
Examiner
Dept. of Chemical Engineering
IITH

Dr. Subha Narayan Rath
Examiner
Dept. of Biomedical Engineering
IITH

Dr. Harikrishnan Narayanan Unni
Adviser
Dept. of Biomedical Engineering
IITH

Declaration

I declare that this written submission represents my ideas in my own words, and where ideas or words of others have been included, I have adequately cited and referenced the original sources. I also declare that I have adhered to all principles of academic honesty and integrity and have not misrepresented or fabricated or falsified any idea/data/fact/source in my submission. I understand that any violation of the above will be a cause for disciplinary action by the Institute and can also evoke penal action from the sources that have thus not been properly cited, or from whom proper permission has not been taken when needed.

Saniya

(Signature)

(Ms. Kshirsagar Saniya Sanjay)

BM16MTECH11005

(Roll No.)

Acknowledgements

I express my sincere gratitude towards my adviser Dr. Harikrishnan Narayanan Unni for his guidance. It wouldn't have been possible without his constant support. I would also like to thank people from Biomicrofluidic lab for their help.

I would like to take this opportunity to thank everyone who has been motivating and supporting me throughout this project.

Abstract

Microfluidic devices have been used in various applications including automated analysis systems, biological applications like DNA sequencing, antigen-antibody reactions, protein studies, chemical applications, single cell studies, etc.

Microfluidic devices are primarily categorised into two types. First are continuous microfluidic devices. These devices consist of predefined microchannels, micro-valves, and syringe pumps. Fluid is continuously flowing in these channels. The second type is digital microfluidic platforms. In this type, MXN array of electrodes is patterned on non-conducting substrate. Fluid is discretized to form tiny droplets. These droplets are transported, mixed and split using external electric field.

Digital microfluidic devices are configurable as there are no permanently etched channels. Also, they have high throughput. Multiple reactions can be performed on the same platform at the same time. The time taken to complete one reaction is less compared to the continuous devices. Thus they help in faster analysis. These devices are controlled by electrical field and thus unlike continuous devices, digital microfluidic devices are free from mechanically moving parts.

Digital microfluidic devices may suffer from charge accumulation due to electrostatic forces. Also, voltage levels applied play an important role. The applied voltage has to be enough to move droplets but should not cause electrolysis of the liquid used. Also voltage switching time between electrodes and frequency applied are important. These parameters can change the mixing quality. In this work, 2D simulations of droplet manipulation due to voltage application, transport and mixing are carried out. Also digital microfluidic device is designed and fabricated to carry out biological mixing experiments.

Contents

List of Figures

List of Tables

Chapter 1

Introduction

1.1 Microfluidics

Microfluidics is a science and technology of processing and analysing low volume ($10^{-9} - 10^{-18}$ litres) of liquids in channels. These channels have dimensions in tens to hundreds of micrometres. Microfluidics extends its application from chemical synthesis and biological analysis to optics and information technology [8]. These devices are compact and low cost. They help in faster analysis. They can be mass manufactured and easily integrated with other analytical tools. In short, microfluidic devices have the ability to replace conventional top bench equipments in chemical synthesis, biology, analytic chemistry, drug screening and diagnostics.

Microfluidic devices can be categorised into two types. The first one is continuous microfluidic devices. In continuous microfluidic devices, liquid samples or reagents flow through microchannels. These devices can be used for mixing two or more analytes, separation of particular cells from group of other cells and trapping and studying single cell, when we consider biological applications. These operations are done passively by manipulating only liquid flow with enhancing channel design or actively using external electric, magnetic, acoustic or optical energies [13].

The second types of devices are droplet based microfluidic devices. Here, the continuous liquid is discretized into smaller packets of droplets. Reactions are done within single droplet which reduces requirement of further reagents. Also, this eliminates contact with the walls. Hence it reduces the chances of adsorption of reagent molecules on solid surface [17]. Droplets are generated inside a microfluidic channel using two immiscible liquids.

Generation of droplets involves viscous shear force and interfacial force. Relation between gener-

ation of droplets and these two forces is given by capillary number which is a dimensionless number.

$$C_a = \frac{\mu v}{\sigma}$$

Where C_a is capillary number, μ is viscosity, v is velocity of flow and σ is interfacial tension. At low capillary number ($Ca < 1$), interfacial force dominates and thus spherical droplets are formed. At high capillary number ($Ca > 1$), due to dominant viscous forces, droplets are deformed. This is done by changing the flow either passively via bifurcations and constrictions or actively using valves and external fields like electric fields [16] [14]. Generally, droplet based continuous microfluidic devices are used for preparing emulsions or encapsulating cells [33].

1.2 Digital microfluidics (DMF) and Electrowetting on dielectric (EWOD)

Although digital microfluidics (DMF) is also a liquid handling technology where liquid is discretized into pico-nano litre droplets to carry out certain reaction, DMF term is generally used when these droplets are manipulated on array of metal electrode using electric voltage rather than in microchannels [21]. Individual droplets can be transported, merged, mixed, split and dispensed from reservoir by applying series of electric potential to metal electrodes.

Lippmann, in 1875, discovered that externally applied voltage to electrolyte and mercury, changed the climb of mercury in a capillary.This phenomenon is called the electrocapillary effect.He hypothesized that the residual charges change the interfacial surface tension between solid and liquid. This hypothesis formed the basis of electrowetting.

When external electric voltage is applied, charge redistribution causes formation of electric double layer due to electrostatic repulsion.Opposite charges accumulated at the boundary tend to pull droplet and hence change interfacial surface tension as shown in fig(1.1). But as there is no barrier for transport of charges at boundary, charges fuse together leading to electrolysis of liquid droplet.

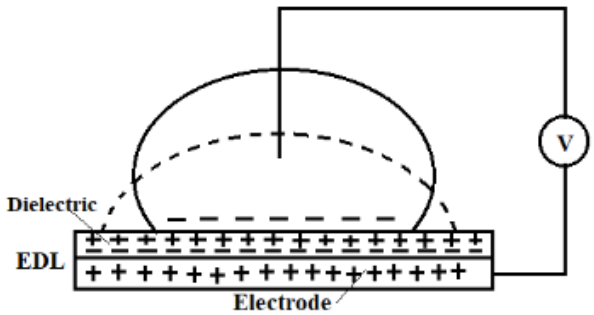

Figure 1.1: Electric double layer

Thus a dielectric layer is introduced between liquid droplet and metal electrode. This dielectric layer acts as an insulator and thus charges do not cross the liquid-solid boundary. This helps to achieve required change in contact angle for electrowetting at low voltages. Thus digital microfluidic devices are coated with dielectric material. These devices are called electrowetting on dielectric (EWOD).

EWOD devices have advantages similar to that of continuous microfluidic devices such as low requirement of reagents and samples, compact size, portability, low cost, mass production and easy integration with analytical devices. But the most important advantage of EWOD chips over other microfluidic devices is flexibility in operations. Use of a particular chip is not limited to certain reaction as there are no permanently etched channels. Different reactions can be performed on single chip with slight changes in software. Also multiplexing reactions is very easy in EWOD chips. If we have M X N array of electrodes, we can perform multiple reactions at the same time. This increases throughput of reaction. Also, after analysis, resultant droplets can be taken to waste without human assistance. Thus EWOD chips are highly automated. Figure (1.2) demonstrates different basic operations that can be performed on chip. These operations include dispensing from reservoirs, transport, merging, mixing, and splitting.

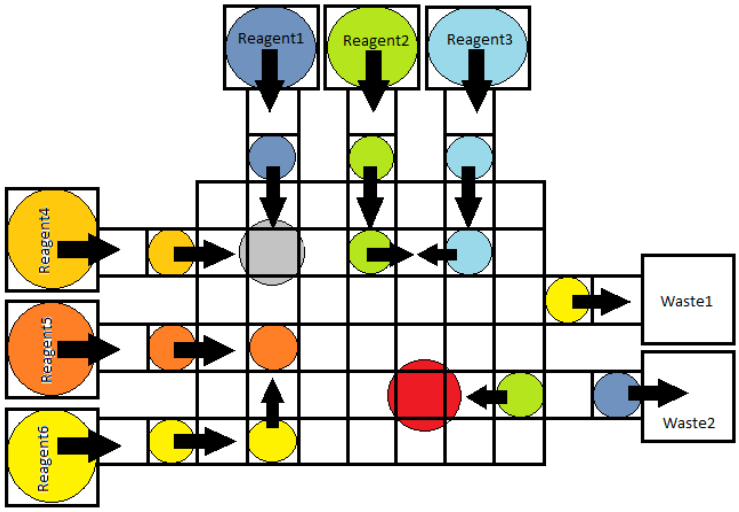

Figure 1.2: Schematics of fundamental operations on MXN electrode array

1.3 Theory of electrowetting

As discussed in section (1.2), EWOD can change contact angle of liquid droplet at low voltage. This phenomenon can be used to dispense, transport, split, merge and mix reagent droplets to carry out multiple biological reactions on single platform. In this work, basic operations like droplet contact angle change, transport of droplets, merging and mixing two droplets are studied.

1.3.1 Contact angle change

External electric field forces overcome surface tension forces which change contact angle of liquid droplet with solid surface as shown in fig1.3. This change in contact angle is given by Young-Lippmann equation.

$$\cos\theta_v = \cos\theta_0 + \frac{\epsilon_0\epsilon_r}{2\gamma_{LG}d}V^2$$

Here in this equation, contact angle after application of voltage is θ_v,$\epsilon_0$is permittivity of free space, ϵ_r and d are permittivity and thickness of dielectric layer respectively. γ_{LG} is surface tension coefficient between liquid and gas and V is voltage applied to electrode.

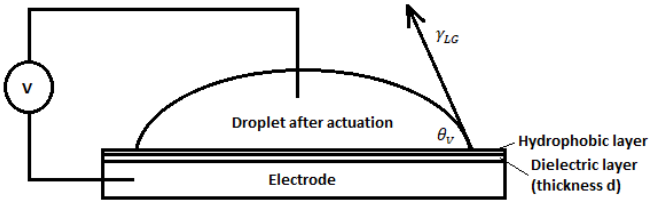

Figure 1.3: Young-Lippmann equation: Contact angle change

Initial contact angle, which is dependent on surface tension coefficients at solid-gas (γ_{SG}), solid-liquid (γ_{SL}) and liquid-gas (γ_{LG}) interfaces, is given by following equation.

$$\cos_\theta = \frac{\gamma_{SG} - \gamma_{SL}}{\gamma_{LG}}$$

Young-Lippmann equation clearly indicates that change in contact angle of a droplet with solid surface is directly proportional to square of voltage applied and inversely to thickness of dielectric layer. For a particular dielectric thickness, voltage levels have to be optimized. Voltage level below than the required level may not induce electrowetting effect in the liquid droplet and voltage above certain level may breakdown the dielectric layer.

1.3.2 Droplet transport

To achieve droplet transport on the electrode array, voltage is switched between electrodes sequentially. When a particular electrode is switched on, due to unbalanced forces at interface, droplet is pulled towards it. Brochards model estimates the velocity of droplet at which it will move towards an adjacent electrode [12].

$$u = \frac{\epsilon_0 \epsilon_r (1 - \cos\theta_v)}{6\mu dl \sin\theta_v} V^2$$

Here ϵ_0 andϵ_r are permittivity of free space and relative permittivity respectively.θ_v denotes contact angle after application of voltage V. μ is viscosity, d is thickness of dielectric layer and l is empirical factor. Application of voltage to electrodes at a time in proper sequence helps to transport multiple droplets and hence carry out different reactions on M X N array of electrodes independently. This increases the throughput of EWOD devices.Fig1.4 demonstrate the basic four operations that can be performed on EWOD devices.

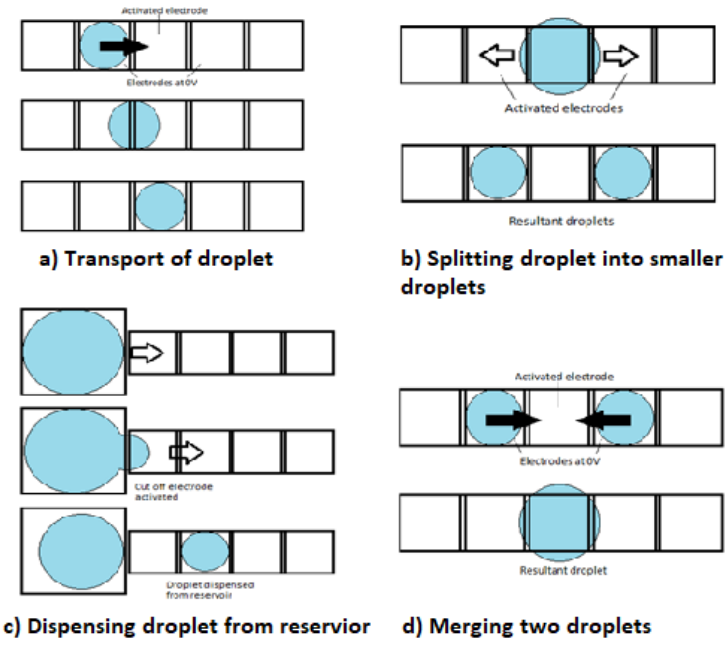

Figure 1.4: Four fundamental operations on chip

1.3.3 Dispensing droplets form reservoir

EWOD devices are capable of dispensing droplets from reservoir on chip. This enables EWOD devices to be totally automated. To dispense smaller droplets from reservoir two electrodes are used. The first one is cut off electrode and the other one is transport electrode. The cut off electrode helps to pinch off the bigger droplet of reagent from reservoir and the transport electrode moves this droplet forward. Proper switching of voltage is required to dispense droplet from reservoir.

1.3.4 Splitting droplets in smaller droplets

When electrodes on the either side of the droplet are actuated, droplet experiences force in opposite directions. This pair of counteracting forces splits the droplet into two smaller droplets. To ensure droplets split perfectly, voltage levels and switching timings have to be optimized.

1.3.5 Merging and mixing of two droplets

EWOD chips can be used to mix two or more reagents efficiently in less time. Droplets are first merged and then transported over electrode array to ensure complete mixing of reagents.

1.4 Applications of EWOD

Reportedly, EWOD has been evolved in last decade extensively [21]. Advantages like rapid reaction and integration with other analytic devices have made EWOD chips possible choice for point-of-care devices. EWOD devices have been used in immunoassays, chemical reactions, enzymatic reactions, proteomics and even cell based applications. Low requirement of reagents and total automation make EWOD devices best suitable for these applications. Also required samples can be prepared through mixing multiple reagents and overall reaction can be analysed on a single chip. Although EWOD devices are still not extensively used, they have potential to contribute significantly in Analytic chemistry, biology and more.

Although EWOD promises to be a near perfect technology, there are a few drawbacks problems that are associated with it. Voltage levels applied to move droplets should be within the threshold level when EWOD devices are used for biological applications. If these levels are above the threshold, they can hamper or degrade biological samples used. Also, accumulation of charges due to electrostatic force and cross talk between electrodes need to be addressed. Other important parameters that affect the correct operation of EWOD devices are switching time of voltage levels between electrodes and frequency of signal applied along with some fabrication challenges.

This work is focused on mixing applications of EWOD devices in biology. To understand electrowetting phenomenon and parameters important in electrowetting, numerical analysis is performed in COMSOL Multiphysics. Our work also addresses the fabrication technique used for EWOD devices for mixing applications. The next chapter is about literature review followed by chapter three discussing about numerical analysis done in COMSOL Multiphysics and chapter four describing fabrication of EWOD device along with electronic circuit design. Finally the fifth chapter concludes this work with results and scope.

Chapter 2

Literature Review

Followed by an elaborate discussion in the first chapter about the electrowetting effect, how it is achieved on dielectric layer at low voltages and its applications, this chapter discusses the motivation behind the presented work. A brief description is provided on the past work performed in the field of numerical analysis of electrowetting, fabrication of EWOD devices and work about droplet routing algorithms.

2.1 Motivatioin: Alkaline phosphatase and Osteoporosis

Alkaline phosphatase (ALP) is an enzyme that helps in breakdown of proteins. It is produced by liver, bone and intestines. Liver is the major producer of ALP-1. Bone produces ALP-2 and intestine produces ALP-3. Alkaline phosphatase (ALP) assay is done to know the condition of these three organs. ALP levels in a person without any diseased condition are 44 to 147 international units per litre. Higher levels of ALP indicate diseased condition of either of these ALP producing organs.

Bone specific alkaline phosphatase (BALP) is isoform of alkaline phosphatase. BAP is a glycoprotein. It is found on membrane of osteoblasts. BALP is considered to be sensitive and reliable indicator for bone metabolism. Osteoporosis is a metabolic disease which is characterized by low bone mass and abnormal architecture of bone. When osteoclasts degrade the bone, due to dissolved calcium, environment becomes acidic. As a response to this acidic environment, levels of alkaline phosphatase increase. Thus higher levels of alkaline phosphatase can be taken as indication of osteoporosis.

Women beginning at age 65 and men at the beginning of age 70 are advised to go for a screening for osteoporosis. Number of women suffering from osteoporosis in India is increasing. Approximately

46 million women are with osteoporosis. This prevalence of osteoporosis in women can be due to low intake of calcium, vitamin D deficiency, early menopause and no access to screening and diagnostic facilities [27].

When it comes to screening patients for osteoporosis using serum ALP as indicator, many traditional methods have been used for decades. These include colorimetry, electrochemistry, fluorescence, chemiluminescence and surface enhanced Raman scattering [34]. These methods are complex in operation. Thus to increase the ease of screening for osteoporosis, microfluidic devices can be used. ALP assay can be performed on chip. The droplets of reagents and blood plasma can be mixed and analysed to know the levels of BALP in the patient.

2.2 Digital Microfluidics

Microfluidic devices have been used in biological applications due to their ability to handle a tiny amount of reagents and samples effectively. Many methods have been used to pump and control fluids through channels. These methods include piezoelectric, electrostatic, electroosmotic, electrophoretic and electromagnetic. But to get rid of mechanical parts like pumps or valves and also permanently etched microchannels to make microfluidic devices more flexible in application point of view, liquid was discretized into microdroplets. Also with advent of microfluidic devices, surface tension force gained attention due to its dominance in microscale [1]. Thermocapillary effect, electrocapillary effect and electrostatic actuation are few methods which were proposed for manipulating droplets. Among these all methods manipulation of surface tension using electrostatic force is the most promising approach.

Digital microfluidic chips are the devices which manipulate surface tension of liquid droplets using external electrostatic force. They require very low amount of sample as well as reagents. They are automated and cost less. Mass production of these devices is easy. Also multiple reactions can be performed at a time on single device. Thus time take for complete screening can be reduced. All these advantages of digital microfluidic devices make them a perfect fit as screening devices[21].

Pollack et al experimentally proved the concept of manipulation of droplets on electrode array [4]. The open channel device fabricated by them had a layer of hydrophobic material on electrode array as insulator. The droplet movement was achieved around 40V. The work proved that the dependency of velocity on voltage is independent of droplet size.

Lee et al in their work proposed the concept of electrowetting on dielectric (EWOD) devices [2]. Cho et al were able to take this concept even further and demonstrate four fundamental operations

successfully[5]. These operations include creating droplet from reservoir,transporting this droplet over the electrode array, mixing and splitting droplets on EWOD device.These applications are important to make EWOD devices suitable for micro total analysis systems (μTAS).The device fabricated by them was a closed channel device. The work highlighted the importance of the distance between the lower and upper plate.All the four operations were achieved at voltage as low as 25V.

Choosing appropriate material and thickness for dielectric layer is important in low voltage EWOD. The required change in contact angle for droplet motion is generally achieved at voltages higher than 100V. Moon et al studied silicon dioxide, parylene and barium strontium titanate (BST) as dielectric material [3].They experimentally proved that droplet can be moved at voltage as low as 15V. Also effect of change in thickness of dielectric layer on EWOD was experimentally studied. Li et al used tantalum pentoxide as dielectric material [11]. They coated EWOD device with 38 nm film of and 16nm thick Teflon AF film. They were able to achieve motion of droplet at 13V.

Despite other materials with high dielectric constants, widely used dielectric material is silicon dioxide due to established chemistry of modification and biofunctionalization of silica based surfaces [15]. Silicon Nitride has all the properties that silicon dioxide possesses. Additionally, silicon nitride is chemically inert to wide range of solvents and has higher dielectric constant and higher dielectric strength than silicon dioxide. Thus silicon nitride is obvious choice as dielectric material in EWOD devices.

EWOD devices are free from any permanently etched channels. These devices can be used for multiple applications just by changing the sequence of applied voltage. These voltage sequences are externally controlled by an electronic circuit.

Pogfoi et al presented study of electrochemical detector using EWOD[19]. The paper discussed about the electronic components like microcontroller and relays used in switching circuits. Najjaran et al, in their paper about ulta-portable smartphone controlled digital microfluidic system, demonstrated the integration of switching circuit with high voltage source [30]. The voltage levels provided by microcontroller are not enough to move the droplets. Thus a high voltage source is integrated with EWOD device. The work elaborately discussed about each part in the electronic circuit used in EWOD systems.

As the EWOD devices are popular due to their ability to perform different reaction on chip at the same time. This multiplexing requires perfect switching of voltage between the electrodes. Droplet routing is critical stage as it is highly complex and has large impact on performance [10]. Thus EWOD devices require sophisticated scheduling algorithms. Yu et al discussed the types of electrode addressing modes and their pros and cons [26]. Also, their work elaborately explained

about problems associated with voltage switching in EWOD devices.

Gupta et al presented an algorithm for coordinating droplet movements in broadcast mode [7]. In the broadcasting addressing mode a set of electrodes is controlled by a single control line. This complicates the routing even more. The work demonstrated that the algorithm is capable of handling multiple reactions at the same time.Pop et al proposed a routing algorithm which implements reactions on chip based on current execution scenario with operation execution time variability [31].

When EWOD devices are used for mixing two reagents, the voltage and switching time for application of this voltage are very important. The quality of mixing depends on the voltage applied. Hence, to know the required voltage levels and switching time, numerical analysis is performed.

The electrowetting phenomenon is due to unbalanced surface tension forces and electrostatic forces. Cahill et al used level set method to simulate Young- Lippmann equation to show droplet manipulation using COMSOL Multiphysics [9]. The problem was designed as two phase laminar flow problem. The first phase was considered to be water and the second phase was air. The work showed that the voltage application to adjacent electrodes moves the droplet interface towards it.

Nahar et al used electrowetting effect as actuation of droplets for cooling of a hotspot [29]. They compared level set and phase field method to track the interface boundary using numerical analysis. The paper discussed all governing equations and boundary conditions given in COMSOL Multiphysics.

Xiong et al demonstrated that the EWOD chip can be used as high throughput droplet dispenser [25]. To convert liquid into discrete droplets dispensers are used as analog to digital converters. To check the functionality and accuracy of proposed device Xiong et al performed numerical analysis in COMSOL Multiphysics. The level set method was used to track the interface.

Vetterling et al simulated multiphase laminar flow problem using two methods [32]. The first method used was modified level set method for more than two phases. The second proposed method used was transport of diluted species method to track the interface of the different phases. The conclusion of this work suggested level set method is the best suitable foe electrowetting simulations. This was because of the incapability of transport of diluted species method in handling surface tension.

A concentration gradient is generated inside a resultant droplet when two droplets with different concentrations are mixed. Dongen et al studied this concentration filed inside ink droplets [22]. The numerical analysis included level set method to track interface of resultant droplet. The concentration field was solved using transport of diluted species to solve the convection- diffusion equation

along with Navier Stokes equation.

This completes the chapter 2 of this thesis. The next chapter is about numerical analysis performed in COMSOL Multiphysics.

Chapter 3

COMSOL Multiphysics: Designs and simulations

To understand the electrowetting phenomenon better, numerical analysis is carried out in COMSOL Multiphysics. COMSOL has multiple physics interfaces along with their governing equations. User can select single or multiple interfaces as per the requirement of problem statement. These interfaces can be linked together to include effect of one parameter on the other. Finally these governing partial differential equations are solved using Finite element method (FEM) by COMSOL.

Here in this section, 2D simulations of Young-Lippmann equation, transport of droplet over an array of electrode and mixing of two droplets with different concentration of analytes are performed. Effects like dielectric thickness and voltage relation, voltage dependency of velocity of droplet, dependency of quality of mixing on voltage are studied.

3.1 Objectives

a. Young-Lippmann equation

   1. Modelling Young-Lippmann equation

   2. Demonstrating reversibility of Lippmann effect

   3. Demonstrating dependency of voltage required for electrowetting on dielectric thickness

b. Single droplet transport

   1. Moving droplet to adjacent electrode

2. Demonstrating dependency of velocity of droplet on voltage applied (Brochards model)

3. Realizing droplet transport over an array of electrodes

c. Droplet merging and mixing

1. Demonstrating merging of two droplets

2. Visualizing concentration field after mixing

3. Demonstrating dependency of mixing quality on voltage applied

3.2 2D simulations of Young-Lippmann equation

As already discussed in section(1.2),droplet changes its contact angle after application of voltage due to unbalanced electric field and surface tension forces. This physical change is given by Young-Lippmann equation. To simulate this phenomenon in COMSOL Multiphysics, Electrostatics (es) and Laminar two phase flow, Moving mesh (tpfmm) interfaces are used [35].

Naiver Stokes equation forms the basis of moving mesh module. It is used to find velocity of liquid-air interface.

$$\rho\frac{du}{dt} + \rho(u.\nabla)u = \nabla.[-pI + \mu((\nabla u) + (\nabla u)^T)] + F$$

$$\nabla.u = 0$$

Here ρ is density, p is pressure, F is any external body force acting on fluid and dependent variable u is velocity.

3.2.1 Setting up COMSOL Multiphysics model

To set up a COMSOL Multiphysics model for 2D simulation of Lippmann-Young equation, electrostatics and laminar two phase flow, moving mesh modules are used. Materials are selected from the library. Time dependent study is chosen to study time dependent changes in droplet shape. Normal meshing size with free triangular meshing elements is used to mesh the geometry. The steps required to set up Multiphysics model are discussed in following sections.

3.2.1.1 Parameters and variables

Initial parameters are set as shown in table (3.1)

Parameters	Notations	Value
Initial contact angle	theta0	120(degree)
Surface tension coefficient	gamma	0.072(N/m)
Relative permittivity of dielectric	er	7.5

Table 3.1: Parameters defined for laminar two phase flow, moving mesh method

Young-Lippmann equation gives angle theta which is declared as a variable and defined as shown in table(3.2)

Variable	Equation	used as
theta	$acos(cos(theta0) + (er * epsilon0_const * V^2)/(2 * d * gamma))$	boundary condition as wetted wall

Table 3.2: Variable defined for laminar two phase flow, moving mesh method

Here voltage V is variable from electrostatics module. This helps to link electrostatic module with laminar two phase flow, moving mesh module.

3.2.1.2 Electrostatic (es) Module

In electrostatic module, voltage levels are provided. Following equations are automatically generated for electric field and electric displacement field.

$$E = -\nabla.V$$

$$D = \epsilon_0 \epsilon_r E$$

Boundary conditions: Zero charge condition is applied to walls.

$$n.D = 0$$

3.2.1.3 Laminar two phase flow, moving mesh (tpfmm) module

Laminar two phase flow, moving mesh interface is defined only in water and air regions. Considering incompressible flow and neglecting inertial term in Navier Stokes equation, physical model is set. Initially velocity field is considered to be zero. Also droplet is exposed to normal atmospheric pressure.

Fluid-fluid interface is defined using following equations where n is normal to interface, T is, σ is M_f is mass fraction and ρ is density.

$$u_1 = u_2$$

$$n_1 T_1 - n_2 T_2 = \sigma(\nabla_t . n_1) n_1 - \nabla_t \sigma$$

$$u_1 = u_2 + M_f [\frac{1}{\rho_1} + \frac{1}{\rho_2}] n_1$$

$$u_{mesh} = u_1 . n_1 - \frac{M_f}{\rho_1} n_1$$

Boundary conditions

No slip boundary condition is given to the boundaries except interface between liquid and solid. Mathematically this condition is given as:

$$u = 0$$

For wall that separates liquid and solid, Navier slip boundary condition is defined as:

$$u.n = 0$$

$$n.T = -\frac{\mu}{\beta} u$$

$\beta$is slip length and n is normal to wall. Navier slip boundary condition allows to define contact angle at liquid-solid interface i.e. $\theta_c = \theta_w . \theta_w$ is calculated by Young-Lippmann equation and is defined as a variable theta. In this way electrostatic module is linked with moving mesh module.

3.2.2 Simulation objectives

3.2.2.1 Demonstration of Young-Lippmann equation

To study the dependence of contact angle on voltage applied, the thickness of dielectric layer is chosen to be 1um. Voltage is varied from 1V to 45 V.

3.2.2.2 Demonstration of reversibility of Lippmann effect

Similar model is set up as discussed in section (). To study reversible effect of contact angle change, 28V is applied from 0.01 s to 0.2 s. Model is studied for 0.4 s.

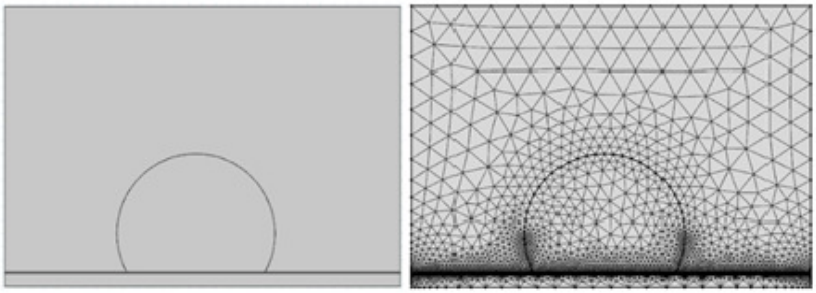

Figure 3.1: Geometry and meshing for Young-Lippmann equation

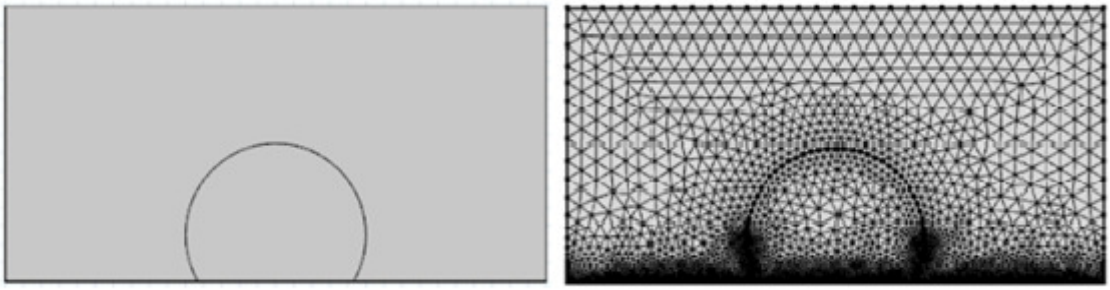

Figure 3.2: Geometry and meshing for reversibility of Lippmann effect

3.2.2.3 Effect of change in thickness of dielectric layer

In Young-Lippmann equation, it is evident that the change in contact angle is inversely proportional to the thickness of dielectric layer. To demonstrate this effect of change in thickness, three different values of thickness, $d = 0.1\mu m, 1\mu m$ and $10\mu m$, are chosen.

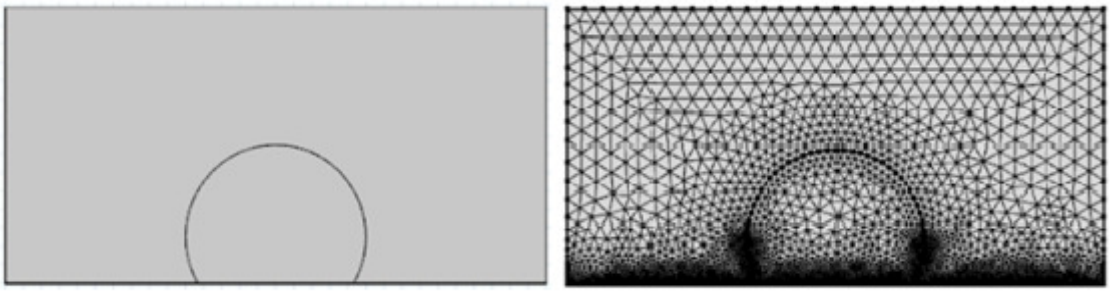

Figure 3.3: Geometry and meshing for Lippmann effect when d=1um

3.3 2D droplet transport

Transport of a droplet over an array of electrodes is achieved by applying sequential voltages to electrodes. When voltage is applied to neighbouring electrode, electric field is generated at the interface of two electrodes. Thus electric force overcomes surface tension force and helps to move the droplet forward.

To model 2D transport of a droplet in direction of applied voltage, conservative two phase laminar flow, level set method is used. This method tracks the interface of two fluids using following set of equations:

$$\rho\frac{du}{dt} + \rho(u.\nabla)u = \nabla.[-pI + \mu((\nabla u) + (\nabla u)^T)] + F$$

$$\nabla.u = 0$$

$$\frac{d\phi}{dt} + u.\nabla\phi = \gamma\nabla.(\epsilon_{ls}\nabla\phi - \phi(1-\phi)\frac{\nabla\phi}{|\nabla\phi|}), \phi = phils$$

Here u is velocity, ρ is the density, p denotes pressure, g is gravitational constant, F_st is surface tension force and F is any external force which acts on volume of fluids.

ϕ is level set variable which is set to be zero in water and 1 in air. Interface is defined by $\phi = 0.5$. γ is reinitialization parameter. Careful selection of this parameter plays an important role in simulation. If value of γ is too small, thickness at the interface cannot remain constant and solution can be affected by numerical instabilities. Also resultant interface can be incorrect if γ is too large. In this work, γ is chosen to be 1.

ϵ_{LS} is parameter controlling the interface thickness. By default, the value of ϵ_{ls} is tpf.hmax/2 where tpf.hmax is dimension of largest meshing element in level set domain. Value of ϵ_{ls} can pose a problem in convergence of the solution if not chosen properly.

Surface tension force is calculated as given in the following equation.

$$F_{st} = \nabla.[(\sigma(I - nn^T))\delta]$$

Where I is the identity matrix, n is the interface normal, σ is the surface tension, and δ is the Dirac delta function that is nonzero only at the fluid interface.

External volume force F in Navier stokes is the same electric force generated by the application

of voltage to electrodes. This electric force is given by divergence of Maxwell stress tensor.

$$F = \nabla.T$$

$$T = ED^T - \frac{1}{2}(E.D)I$$

E defines electric field and D defines electric displacement field.

$$E = -\nabla.V$$

$$D = \epsilon_0 \epsilon_r E$$

For 2D simulation we can reduce components of T as follows.

$$\begin{bmatrix} T_{xx} & T_{xy} \\ T_{yx} & T_{yy} \end{bmatrix}$$

After substituting variables equations, we can write Maxwell stress Tensor as:

$$\begin{bmatrix} \epsilon_0\epsilon_r E_x - \frac{1}{2}\epsilon_0\epsilon_r((E_x)^2 + (E_y)^2) & \epsilon_0\epsilon_r E_x E_y \\ \epsilon_0\epsilon_r E_x E_y & \epsilon_0\epsilon_r E_y - \frac{1}{2}\epsilon_0\epsilon_r((E_x)^2 + (E_y)^2) \end{bmatrix}$$

Where ϵ_r is relative permittivity which is defined in fluid regions and given by the following equation.

$$\epsilon_r = \phi\epsilon_{r1} + (1 - \phi)\epsilon_{r2}$$

This equation directly links electrostatic module to level set module.

3.3.1 Setting up COMSOL Multiphysics module

To set up the COMSOL Multiphysics model for transport of droplets, 2D geometry is used. Electrostatics and Laminar two phase flow, level set modules are selected from the list. A phase initialization, time dependent study is chosen. Parameters and variables are defined. Materials are chosen from the library. Each module has already set up governing partial differential equations. Suitable initial conditions and boundary conditions are given. Geometry is meshed with normal mesh with free triangular elements. At the last phase initialization is done only for level set method and both electrostatics and level set modules are solved in time dependent solver. All these steps

are elaborately discussed in following sections.

3.3.1.1 Parameters and variables

To solve governing partial differential equations of electrostatics and laminar two phase flow, level set (tpf) method, variables like contact angle of the liquid droplet with solid wall, volume forces acting on the liquid droplet and permittivity of region where level set method is applied have to be specified. To specify these variables, certain parameters have to be defined. These parameters and variables are listed in table (3.3) and table (3.4) respectively.

Parameters	Notations	Value
Initial contact angle	theta0	120(degree)
Surface tension coefficient	gamma	0.072(N/m)
Relative permittivity of dielectric	er	7.5
Permittivity of water	$perm_water$	80
Permittivity of air	$perm_air$	1

Table 3.3: Parameters for Laminar two phase flow, Levels set method

Variable	Expression
theta	$acos(cos(theta)+(er*epsilon_0*V^2)/(2*gamma*d))$
$epsilon_r$	$tpf.Vf1 * perm_water + tpf.Vf2 * perm_air$
T11	$-epsilon0_const * (epsilon_r/2 * (es.Ex^2 + es.Ey^2) - epsilon_r * es.Ex^2)$
T12	$epsilon_0 * epsilon_r * es.Ex * es.Ey$
T21	$epsilon_0 * epsilon_r * es.Ex * es.Ey$
T22	$epsilon_0*(epsilon_r/2*(es.Ex^2+es.Ey^2)-epsilon_r* es.Ey^2)$
fx	$d(T11, x) + d(T12, y)$
fy	$d(T21, x) + d(T22, y)$

Table 3.4: Variables defined for laminar two phase flow, level set method

3.3.1.2 Electrostatics module (es)

As discussed already, all the required equations are already set up by COMSOL. Voltage is externally provided. Time varying voltage is applied to each electrode. Thus electric field generated at particular electrode exerts volume force f_x and f_y on droplet and pulls droplet towards it.

Boundary condition

Zero charge boundary condition is applied to all walls. It is given as $n.D = 0$. n denotes normal to the surface and D is the displacement field.

3.3.1.3 Two phase laminar flow, level set method (ls)

Only water and air regions are selected in this module. All governing equations are set up as discussed in section(). Water is chosen to be fluid 1 and air as fluid 2. Volume forces f_x and f_y are applied to both water droplet and air.

Boundary condition

Boundary at solid- liquid interface is defined as wetted wall condition. Angle with wall is denoted by θ_w and is given by variable theta. This theta is the angle given by Young-Lippmann equation.

3.3.2 Simulation of objectives

3.3.2.1 Droplet motion to adjacent electrode

Droplet moves towards adjacent activated electrode due to generated electric force at the interface. To simulate this effect, electrostatics (es) and laminar two phase flow, level set method (tpf) modules are used. Geometry used for this simulation is shown in figure (3.4). Electrodes are $3mm0.1mm$ in size and dielectric layer is 1m thick. The middle electrode is activated with 28V.

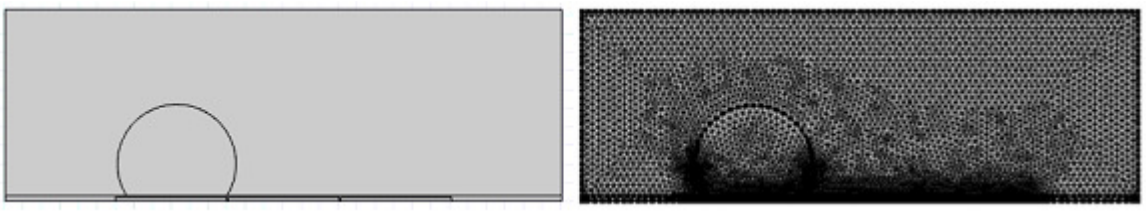

Figure 3.4: Geometry and meshing for droplet transport to the adjacent electrode

3.3.2.2 Transport of a droplet over an array of electrodes

Switching voltage between electrodes moves the droplet over the array. This switching has to be optimized for seamless transport of the droplet. To study this switching of voltage between electrode, electrostatics and level set method modules are used. Geometry for this simulation contains an array of five electrodes with a dielectric layer. Electrode size is 3mm X 0.1mm. Electrodes are activated with 28V rectangular pulses.

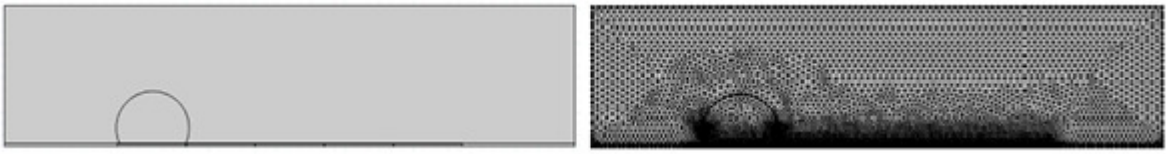

Figure 3.5: Geometry and meshing for droplet transport over an array of electrodes

3.3.2.3 Voltage dependency of droplet velocity

According to Broachards model, velocity of droplet has strong dependence of applied voltage. This relation is given as:

$$u = \frac{\epsilon_0 \epsilon_r (1 - \cos\theta_v)}{6\mu dl \sin\theta_v} V^2$$

Thus to study this dependency, a COMSOL model is set up.

Geometry includes array of three electrodes and layer of dielectric. Electrodes are $3mmX0.1mm$ in size. Dielectric layer thickness is set to $1\mu m$ and $0.1\mu m$.

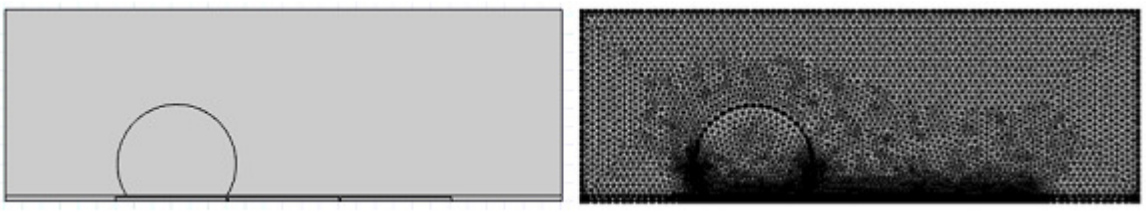

Figure 3.6: Geometry and meshing for demonstration of Brochard's model

Middle electrode is actuated with voltage V while both corner electrodes are at 0V.Model is simulated at 16V, 20V, 24V, 28V and 32V for 1m dielectric layer.

3.4 Merging and mixing two droplets

Droplet merging is one of the important basic applications in EWOD. Droplets of single or multiple solutions can be merged and mixed effectively in lesser time. To simulate the droplet merging and mixing, Electrostatics (es), two phase laminar flow, level set (tpf) and transport of diluted species (tds) modules are used. Electrostatics module provides required electric force. Level set method tracks interface along with Navier Stokes equation and transport of diluted species use convection-diffusion equation to obtain concentration of analytes within resultant droplet.

3.4.1 Setting up COMSOL Multiphysics model

To study 2D simulation of mixing of two droplets, electrostatics (es), laminar two phase, level set method (tpf) and transport of diluted species (tds) modules are used. All the boundary and initial conditions for electrostatics and laminar two phase flow, level set method are the same as discussed in section (3.3). In this section transport of diluted species module is described.

3.4.1.1 Transport of diluted species (tds)

Transport of diluted species (tds) module uses convection-diffusion equation to solve for concentration field inside a droplet. The convection diffusion equation is given by the following equation.

$$\frac{dc}{dt} + u.\nabla c - D.\nabla^2 c = 0$$

Here c represents concentration, u is velocity and D is diffusion constant. Velocity used in convection-diffusion equation is taken from laminar two phase flow, level set (tpf) module. But to link level set module and transport of diluted species module, we have to set diffusivity as a function of level set variable.

For simulation of convection-diffusion equation, convection is selected as transport mechanism. Velocity field is chosen from level set module. One droplet has concentration equal to $1mol/m^3$ and other one at $0mol/m^3$. Diffusion coefficient for water-air pair is defined as $10^-50m^2/s$ and for water- water pair as $10^-9m^2/s$.

Boundary conditions

No flux boundary condition is applied to all the boundaries of the geometry except boundaries separating water droplets from air.

$$-n.N = 0$$

3.4.2 Simulation of objectives

3.4.2.1 Merging two droplets and transporting resultant droplet

To study the merging of two droplets and transport of resultant droplet, electrostatics (es) and laminar two phase flow, level set method modules are used. The electrode array has five $3mmX0.1mm$ electrodes. Two droplets are located either sides of activated electrode which is the third electrode of the array. This electrode is given 28V for 0.2s. Once both the droplets are merged, resultant droplet is transported to the fourth electrode. This fourth electrode is activated from 0.2s to 0.55s.

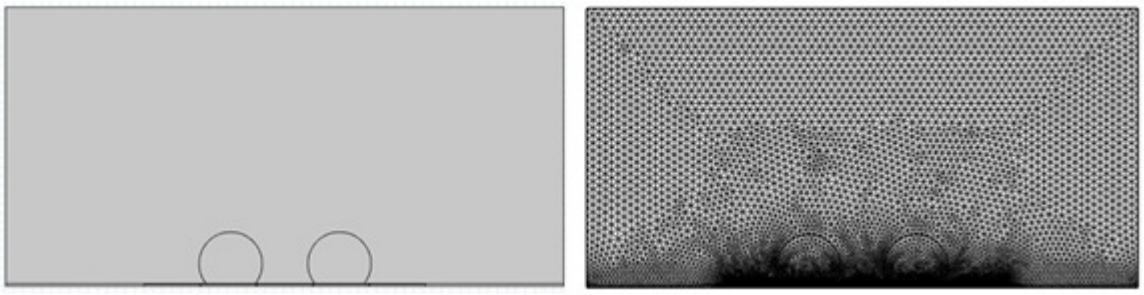

Figure 3.7: Geometry and meshing for merging of two droplets

3.4.2.2 Mixing and concentration field

Two droplets are merged and mixed at 28V. Concentrations of individual droplets are set at $1mol/m^3$ and $0mol/m^3$. Concentration field inside the resultant droplet is calculated using CD equation.

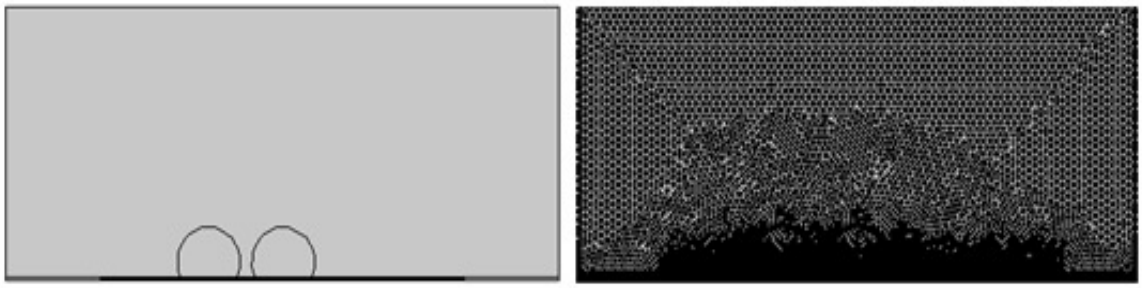

Figure 3.8: Geometry and meshing for concentration field studies

3.4.2.3 Demonstration of quality of mixing on voltage

To check voltage dependency of quality of mixing, simulation is carried out at 16,20,24,26 and 28 V. two droplets are placed one electrode apart. The electrode array has five electrodes. The middle electrode is applied 28V. Rest of the electrodes are at 0V. One droplet has concentration $1mol/m^3$

and the other has $0mol/m^3$.

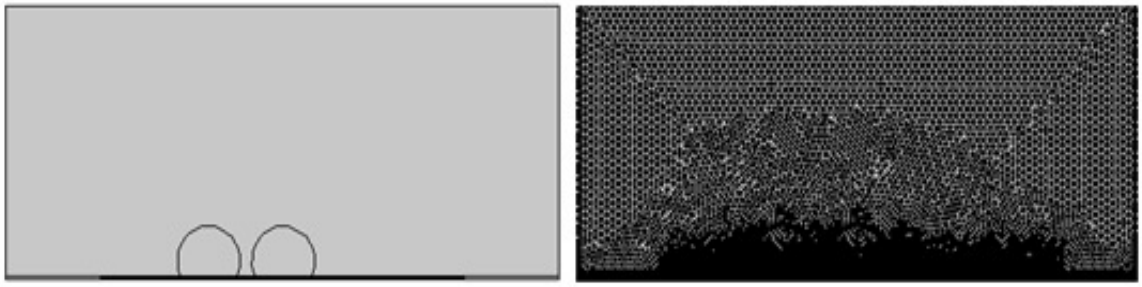

Figure 3.9: Geometry and meshing for quality of mixing studies

This completes the numerical analysis for electrowetting and mixing of two droplets of reagents. These parameters help us in understanding the effects of different parameters on electrowetting of a liquid droplet, its transport over an electrode array and mixing efficiency. The next chapter gives in sites about fabrication technique and electronic circuit design.

Chapter 4

Design and fabrication of EWOD device and electronic switching circuit

Design and fabrication of EWOD chip and switching circuit When we talk about EWOD devices as a system, it is intended that it includes the fabricated electrode array chip and an electronic switching circuit which controls the sequence of voltage from external source. In this section, design and fabrication of EWOD chip and electronic switching circuit are discussed.

4.1 Fabrication of the EWOD device

Electrowetting on dielectric devices are categorized into open channel and closed channel devices [20]. The open channel devices have an array of electrodes fabricated on an insulating substrate. A dielectric and a hydrophobic layer are coated on the top of this array. A liquid droplet is placed on the top of this hydrophobic layer surrounded by air.

Proposed EWOD device is a closed channel device. It has a top and a bottom plate. Liquid droplet is sandwiched between these two plates. The top plate gives additional stability to droplet and helps in splitting droplets in smaller ones [6]. Also it reduces voltage required to move droplets.

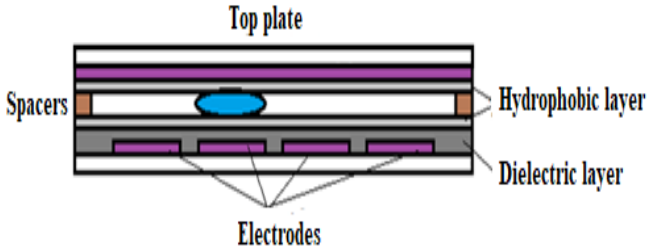

Figure 4.1: Schematic representation of the proposed EWOD device

The bottom plate will carry actuating electrodes and the top plate will carry continuous ground electrode. Bottom plate will be coated with dielectric as well as hydrophobic materials. Whereas top plate will be coated with only hydrophobic material as shown in fig.(4.1). Fig.(4.1) shows schematics of EWOD device with both bottom and top plate. Gap between bottom and top plate is defined by spacers. Here glass cover slips are used as spacers.

4.1.1 Design of the EWOD device

The bottom plate is designed in AutoCAD. Fig(4.2) is schematics of design. There are 21 control electrodes. These 21 electrodes include 12 actuating electrodes, 6 cut off electrodes and 3 reservoirs. Actuating electrodes help to transport droplets. Cut off electrodes help in dispensing droplets from reservoirs.

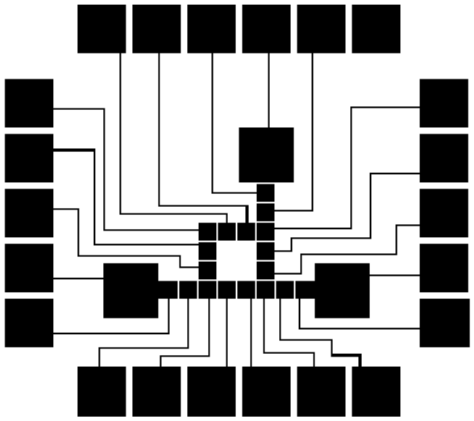

Figure 4.2: AutoCAD design

Each electrode is connected to one contact pad located at the periphery. These contact pads are used for connecting the EWOD device with external electronic circuit. All dimensions are listed in table (4.1).

1	Electrodes	3mm X 3mm
2	Gap between the electrodes	300um
3	Reservoirs	9mm X 9mm
4	Contact pads	8mm X 8mm
5	Gap between contact pads	1mm
6	Thickness of wires connecting electrodes and contact pads	500um

Table 4.1: Design Parameters

4.1.2 Fabrication process

Fabrication of EWOD device includes metal electrode patterning on substrate, deposition of dielectric material and finally coating the chip with hydrophobic material.

4.1.2.1 Electrode Patterning

Electrode patterning is done using photolithography technique. Glass coated with Indium Tin Oxide (ITO) is used as substrate. The process of patterning is shown in fig.(4.3)

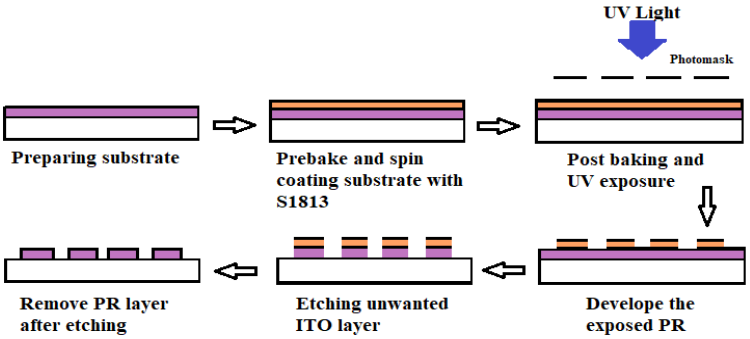

Figure 4.3: Flow chart for electrode patterning process

1. The first step in this process is cleaning the substrate. Substrate is sonicated for 5 minutes. This helps to remove dust particles present on the surface of ITO glass. Once sonication is done, ITO glass is washed with Acetone and deionized water.

2. Cleaned ITO glass is then prebaked at 110 for 90s. This improves the adherence of photoresist. A positive photoresists S1813 is used in this process. Positive photoresists undergo changes in chemical structure when exposed to UV light. Thus becomes more soluble to developer.

   S1813 is less viscous solution. Maximum thickness that can be achieved by one round of spin coating is 3m. Therefore to coat 5m thick resist, two rounds of spin coating are done.

3. Prebaked ITO glass is coated with S1813. Spin coating is done at 500 RPM for 1 min. followed by 3000 RPM for 30 sec.

4. This coated ITO glass is then baked at 110 for 90 sec. Glass is allowed to cool down and same procedure of spin coating is followed for one more time.

   Baking after first coat allows coated photoresist to settle. This avoids dissolving first layer into second one.

5. When two rounds of spin coating are done, ITO glass is baked at 110 for 90 sec. This is known as post baking.

6. Now this photoresist coated ITO glass is loaded into UV writer. Photomask is aligned properly. Power of UV writer is set to 80Once this exposure is done, ITO glass is baked again at 110 for 90 sec.

7. The substrate is then developed using MF-CD 26, a developer specific to S1813. The developer dissolves all the exposed resist.

8. To remove unwanted ITO from glass substrate, etchant is prepared. Etchant is a solution which dissolves metal. Here solution of FeCl3 in HCl and water is used. 7g of FeCl3 is dissolved in 50 ml of HCl in water solution completely.

   ITO glass is dipped inside this etchant for 6min. Continuous shaking is required to insure even etching of unwanted ITO.

   Etching time is crucial parameter because less etching causes fused electrodes whereas excess time may cause tiny holes in electrodes.

9. Once etching is done perfectly, patterned ITO glass is washed with deionized water, acetone and again with DI water.

Multiple chips are fabricated to check reproducibility of this protocol. Fig.(4.4) shows patterned ITO glass with coated silicon nitride.

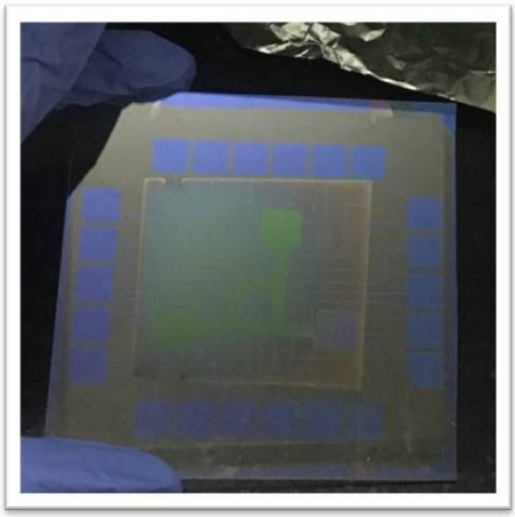

Figure 4.4: Fabricated device

Electrode insulation is important for low voltage electrowetting. To insulate patterned ITO electrodes from liquid droplet, EWOD device is coated with dielectric and hydrophobic layers.

4.1.2.2 Dielectric coating

When any dielectric material is considered to be coated onto EWOD chip, certain characteristics are taken into consideration. The first and the most important characteristic of any material is dielectric constant. As Young-Lippmann equation proves, higher the dielectric constant, lower is the required actuation voltage. The second property is ability of material to form a thin layer. This is important as higher thickness of dielectric material requires higher voltage to actuate the liquid droplet. Then properties like hydrophobicity and transparency are considered.

Silicon nitride (Si_3N_4) has dielectric constant near 7.5. It can be sputtered to give thin films ranging in nanometres. Thus silicon nitride is chosen as the dielectric layer. To coat fabricated EWOD devices with dielectric layer, silicon nitride is sputtered onto them.

Also to study properties of different materials as an option for dielectric layer, unpatterned ITO glass is coated with SU8 photoresist and polydimethylsiloxane (PDMS)[23].

4.1.2.3 Hydrophobic coating

Teflon AF solution is coated on the top of dielectric layer. The Teflon is spin coated at 500 rpm for 30s and 4000 rpm for 60s. This Teflon coated EWOD device is heated at 200 for 10 min.

Also top plate of EWOD device carries a continuous ground electrode. To ensure smooth and friction free transport of droplet over an electrode array, top plate of the fabricated device is coated with Teflon solution. Teflon is spin coated over unpatterned ITO glass at 500 rpm for 30s and 4000 rpm for 60s. This spin coated ITO glass is then heated at 200 for 10min.

4.2 Electrode addressing

Application of voltage to correct electrode ensures seamless and accurate motion of droplets on EWOD platforms. Application of voltage to a particular electrode as per the predefined sequence is known as electrode addressing [24].

Fundamentally there are two types of electrode addressing techniques. The first one is called the direct addressing mode. In this technique, each electrode is connected with an independent control pin. This increases flexibility in control over the electrodes. One major drawback in direct addressing mode is the increased requirement of control pins. The second addressing technique is broadcast addressing. In broadcast addressing, one control pin is shared with two or more electrodes. This reduces the number of required control pins, but at the cost of losing flexibility in control.

As the microfluidic chip is fabricated using single layer fabrication technique, direct addressing mode is implemented for electrode addressing in this work.

4.2.1 Microcontroller

The control over time varying electric potential is provided by a microcontroller. A microcontroller is a small computer with processors, memory and input-output peripherals. A predefined sequence is fed into processor of the microcontroller, for each electrode. Output ports are used for physical connection between microcontroller and EWOD chip. Arduino mega 2560 serves the purpose of microcontroller. It has 54 digital I/O pins which are enough to control 21 electrodes independently. A software program is written in open source Arduino software (IDE) to programme the microcontroller according to required operations.

4.2.2 Switching circuit

The voltage required for performing basic operations like transport, mixing, merging is in the order of tens of volts. Output voltage given by Arduino Mega 2560 is 5V. Thus, the electric voltage obtained from Arduino Mega cannot be used directly. A high voltage source is required to provide the sufficient voltage. Therefore, it is necessary to have a switching circuit which will connect high voltage source to electrodes but with some control.

This can be achieved by using relays. Relays act like an open switch. They are used to control a circuit by a separate low-power signal. To address this, an output signal from microcontroller can be used to operate relays. Once a particular relay is closed, high voltage source is connected to the electrode. This particular electrode will then be activated.

4.2.3 Relays

Mechanical relays are susceptible to wear and tear due to their moving parts. This ultimately reduces their stability and life. Also, they suffer from low switching speed. The contact bounce may affect the circuit that is connected to the relays. On the other hand, solid state relays which are electronic switching circuits, work without any moving parts. They are switched ON and OFF when a small external voltage is applied across the control terminals. They have slimmer profile than mechanical relays. Switching is faster in solid state relays as compared to mechanical relays. As they are free from any form of moving parts, their operation is silent. The solid state relays also have an increased lifetime. Thus, the solid state relays are a better option than the mechanical relays.

4.2.4 Metal oxide field effect transistor (MOSFET)

MOSFET is voltage controlled semiconductor device. It has three terminals named as Gate, Source and Drain. The gate is supplied by an external voltage. If this voltage is greater than the threshold voltage of MOSFET, it allows current to pass through it. Thus it perfectly works as a switch.

Here due to higher voltage requirement, MOSFET BSS 123 is chosen. The voltage handling capacity of this MOSFET is 100V. Also continuous drain current that it can sustain is 150mA. Thus BSS123 is perfect choice as switch in this case.

4.2.5 Connections

Gate of MOSFET receives signal from Arduino, source is grounded and drain is connected to high voltage source. The voltage source is connected to drain through a 10Kohm resistor which lim-

its current passing through MOSFET. Electrodes will be connected across MOSFET as shown in fig(4.5).

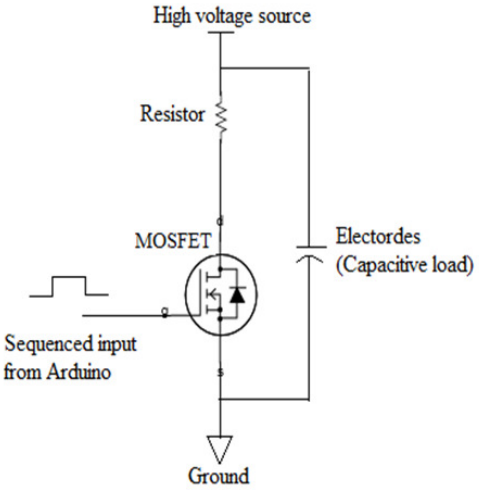

Figure 4.5: Schematics of connections to MOSFET

When signal from Arduino crosses threshold voltage at the Gate, MOSFET starts conducting. Connection is established between source and drain. Current starts flowing through resistor and MOSFET. Electrodes act as capacitive load connected across this circuit. Due to the connections done, entire potential drop appears across the electrode. Fig.(4.6) demonstrates each component that completes the switching circuit.

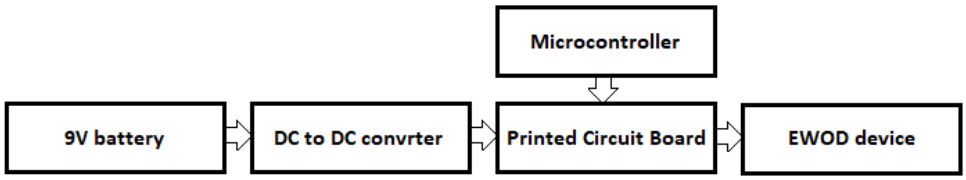

Figure 4.6: Block diagram of electronic circuit

4.2.6 PCB design

To control one electrode in direct addressing mode, we require one MOSFET and one resistor. We have 21 electrodes in proposed design of EWOD chip. Therefore 21 MOSFET and 21 resistors were mounted on a printed circuit board. The PCB is designed in software called Eagle by Autodesk.

PCB is fabricated using single layer fabrication technique. Dimensions of fabricated PCB are 13cm X 6cm. Connections of PCB and layout of PCB designed in Eagle are shown in fig.(4.7) and fig.(4.8) respectively.

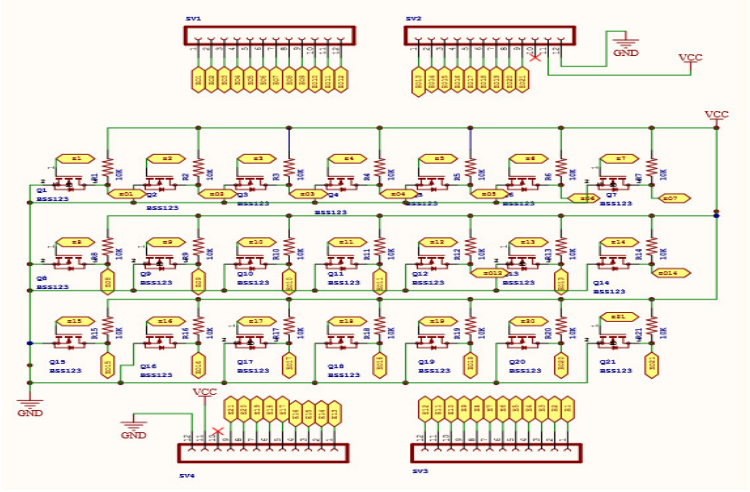

Figure 4.7: Schematics of connections to MOSFET

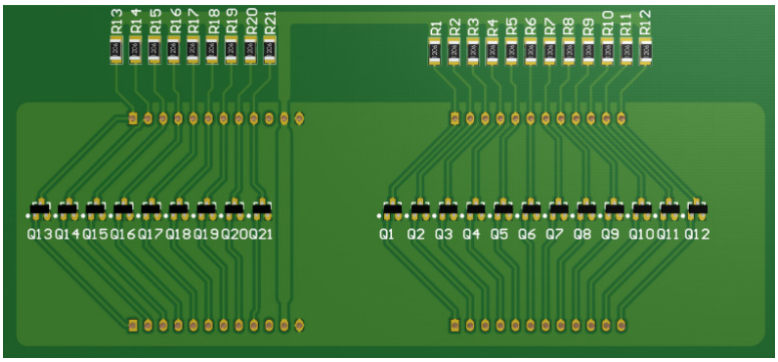

Figure 4.8: Layout of PCB

4.3 Designed experiments

After complete fabrication of EWOD chip, the device is integrated with electronic circuit. To check electrowetting phenomenon, droplets of KCl (15mS), PBS (5.8mS) and DI (0.1mS) water will be placed over the electrodes. A silver nitride wire, which acts as ground electrode, will be dipped inside these droplets. Voltage applied to electrodes will be increased gradually to observe change in contact angle. This experiment will be carried out for chips coated with silicon nitride, SU8 and PDMS.

Once contact angle change is observed, these droplets will be placed on electrodes with 0V applied to them. The neighbouring electrode will be activated. The activation voltage will be kept as low as possible and will be gradually increased to note the threshold voltage for droplet transport.

After achieving droplet motion, this device will be used to efficiently mix two liquid droplets. Once the mixing is achieved, the device can be used to mix blood plasma with BCIP disodium salt and Nitro blue tetrazolium. This reaction changes blood plasma colour from pale yellow to dark purple [34].

Chapter 5

Results and conclusion

This chapter demonstrates the results achieved after numerical analysis in COMSOL Multiphysics and experiments performed on fabricated EWOD device. The first part of this chapter discusses about the simulation results for Young-Lippmann equation, droplet transport and mixing on chip. It also comments on the dependency of electrowetting operations on different parameters. The second part in this chapter is about results obtained after performing experiments on fabricated EWOD device.

5.1 Numerical Analysis in COMSOL Multiphysics

To understand the electrowetting, transport of a liquid droplet over an array of electrodes and mixing of two liquid droplets, numerical analysis is performed in COMSOL Multiphysics. The Young- Lippmann equation is simulated using electrostatics and laminar two phase flow, moving mesh. Dependency of contact angle on applied voltage, reversibility of Young-Lippmann effect and dependency of contact angle on thickness of dielectric are studied. The droplet transport is done using electrostatics and laminar two phase flow, level set method whereas the concentration field after mixing is visualized using transport of diluted species. Dependency of velocity and efficiency of mixing on voltage are studied. The following sections elaborately describe the results of these simulations.

5.1.1 Modelling Young-Lippmann equation

The Young-Lippmann equation calculates the contact angle of a liquid droplet after voltage application. The equation also states that the contact angle change is proportional to the square of applied

voltage. To model this equation in COMSOL Multiphysics, Laminar two phase flow, moving mesh and electrostatic modules are used. The initial contact angle of droplet is 120. The voltage applied to the droplet is gradually increased from 1V to 45V. Using boundary probe, contact angle of droplet with solid surface is calculated at each step. The contact angle change is significant after 17V which can be seen in fig(5.1). All the values are plotted in fig(5.2). The values of change in contact angle are listed in table (5.1)

Applied voltage(Voltage)	Contact angle(Degree)	Change in contact angle(Degree)
0	120	0
1	119.971	0.0291
5	119.24	0.76
9	117.588	2.41
13	115.0327	4.96
17	111.623	8.377
21	107.418	12.58
25	102.45	17.55
29	96.44	23.55
33	89.874	30.126
37	82.454	37.54
41	74.026	45.97
45	64.286	55.71

Table 5.1: Values of voltage and respective contact angle and relative change

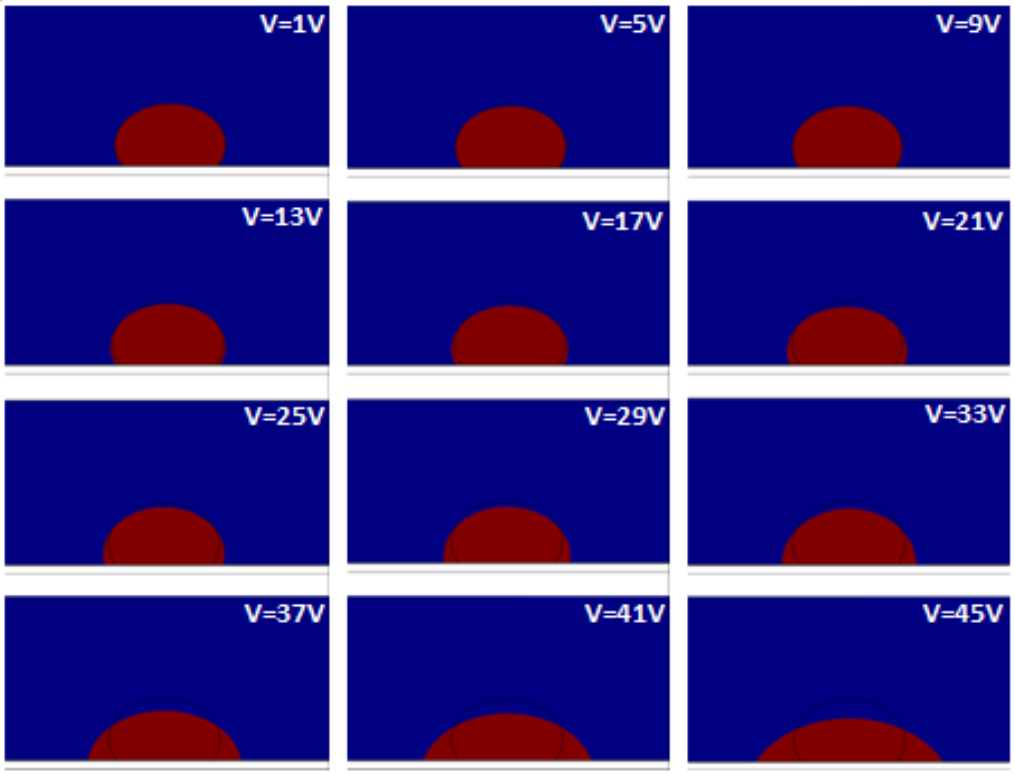

Figure 5.1: Change in contact angle of the droplet at different voltage levels

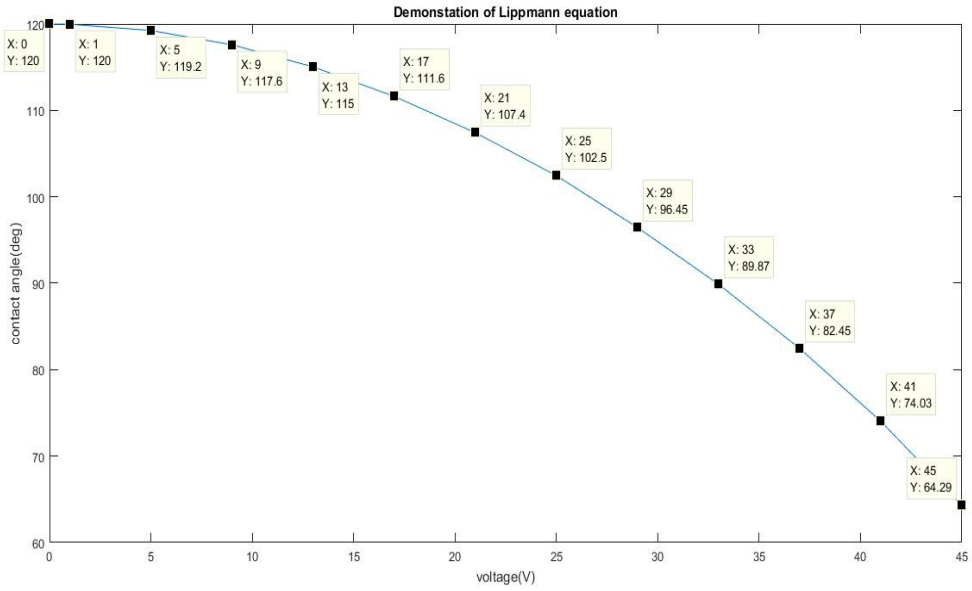

Figure 5.2: Graphical representation of change in contact angle at different voltage levels

5.1.2 Reversibility of Lippmann effect

As already discussed, a liquid droplet changes its contact angle when voltage is applied to it. To check reversibility of this effect, a simulation is performed in COMSOL Multiphysics using electrostatics and laminar two phase flow, moving mesh modules. A water droplet is located on dielectric film. The electrode beneath this dielectric layer is activated with 28V at 0.01s. The contact angle of this droplet changes to 98 from 120. The voltage source is switched off at 0.20s. Once the voltage source is switched off, the droplet bounces back and tries to regain the original shape with contact angle of 120. This shows the Young-Lippmann effect is reversible. Fig(5.3) shows shape of the droplet at different time frames.

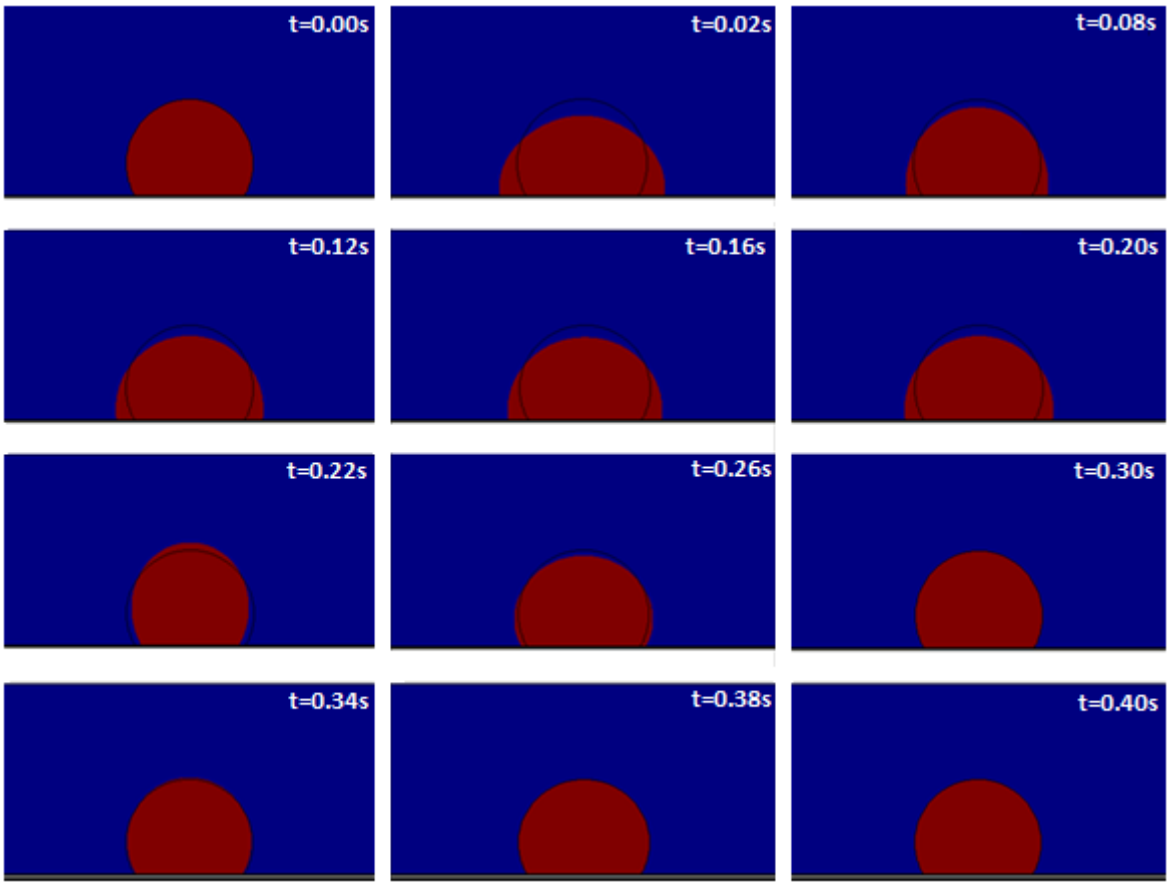

Figure 5.3: Reversibility of Lippmann effect

d=0.1μm		d=1μm		d=10μm	
voltage(V)	$\Delta\theta$(deg)	voltage(V)	$\Delta\theta$(deg)	voltage(V)	$\Delta\theta$(deg)
0	0	0	0	0	0
6	10	18	9.4	60	10
8	18	26	19	85	20
10	27.5	34	31.6	105	
12	38	38	40	120	39
14	53.2	46	58	150	61.7
16	72	50	73	160	71.9

Table 5.2: Contact angle change for dielectric thickness values d=0.1um, 1um and 10um

5.1.3 Demonstrating dependency of voltage required for electrowetting on dielectric thickness

The contact angle change in a liquid droplet is inversely proportional to the thickness of dielectric layer. Therefore the voltage requirement for achieving certain change in contact angle is different for different values of dielectric thickness. To verify this statement, three values are chosen. The dielectric constant and initial contact angle are constant in all three cases. When the thickness of dielectric layer is 0.1m, voltage is increased gradually from 6V to 16V. Using boundary probe, contact angle is plotted at each voltage. Similarly, when values of the thickness of dielectric layer are 1m and 10m, voltage is varied from 18V to 50V and 60V to 160V respectively. The boundary probe is used to record the value of contact angle at each voltage. The contact angle changes for each value of dielectric thickness are listed in table (5.2). It is evident from these values that lower the dielectric layer, lesser is the required voltage.Fig(5.4), fig(5.5) and fig(5.6) demonstrate the contact angles at different voltages when d=0.1um, 1um and 10um respectively. Also fig(5.7) graphically represent contact angle changes in these three different cases.

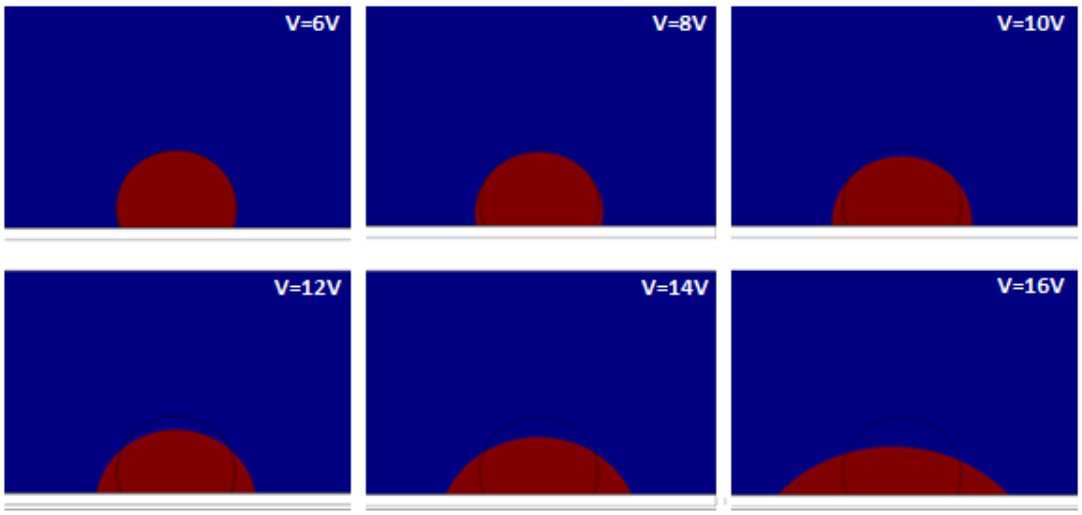

Figure 5.4: Change in contact angle of the droplet at different voltage levels when d=0.1um

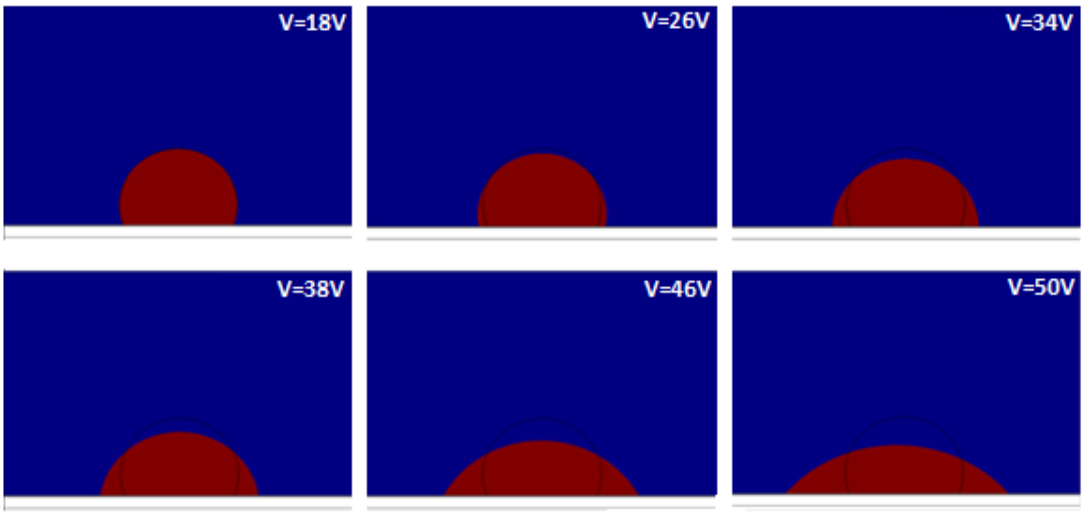

Figure 5.5: Change in contact angle of the droplet at different voltage levels when d=1um

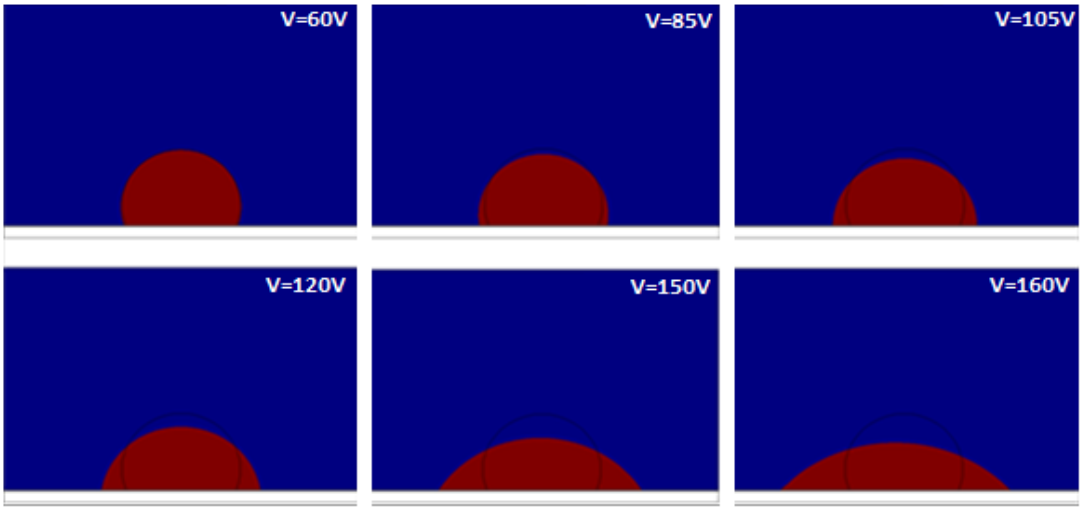

Figure 5.6: Change in contact angle of the droplet at different voltage levels when d=1u0m

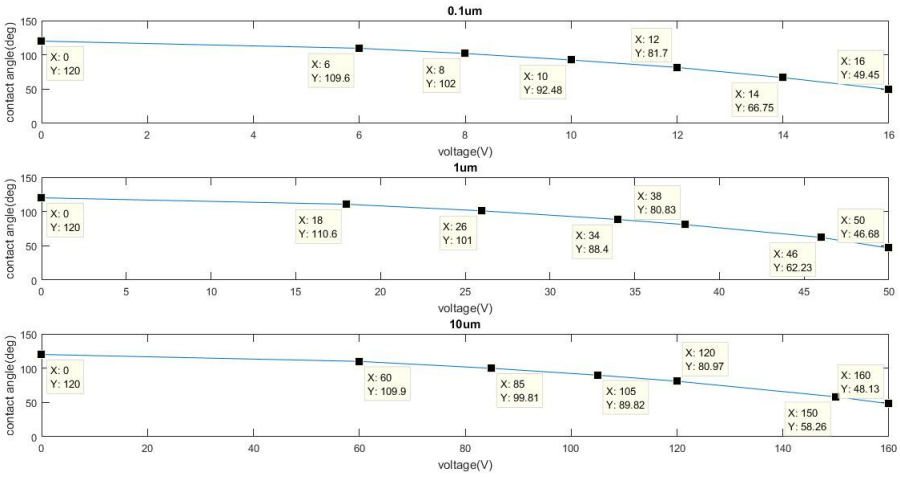

Figure 5.7: Graphical representation of change in contact angle of the droplet at different voltage levels when d=0.1um,1um and 10um

5.1.4 Moving droplet to adjacent electrode

Droplet transport is one of the fundamental operations performed on EWOD devices. The electric field exerts force on a droplet and helps it to overcome the surface tension forces. Therefore, the droplet moves towards the electric field.

To study this phenomenon, a COMSOL model is built up using electrostatics and laminar two phase flow, level set method. The droplet is located at the first electrode in an array of three

electrodes. 28V are supplied to the middle electrode. The droplet transport is completed in 0.056s. Fig (5.8) shows stages of droplet transport at different time frames.

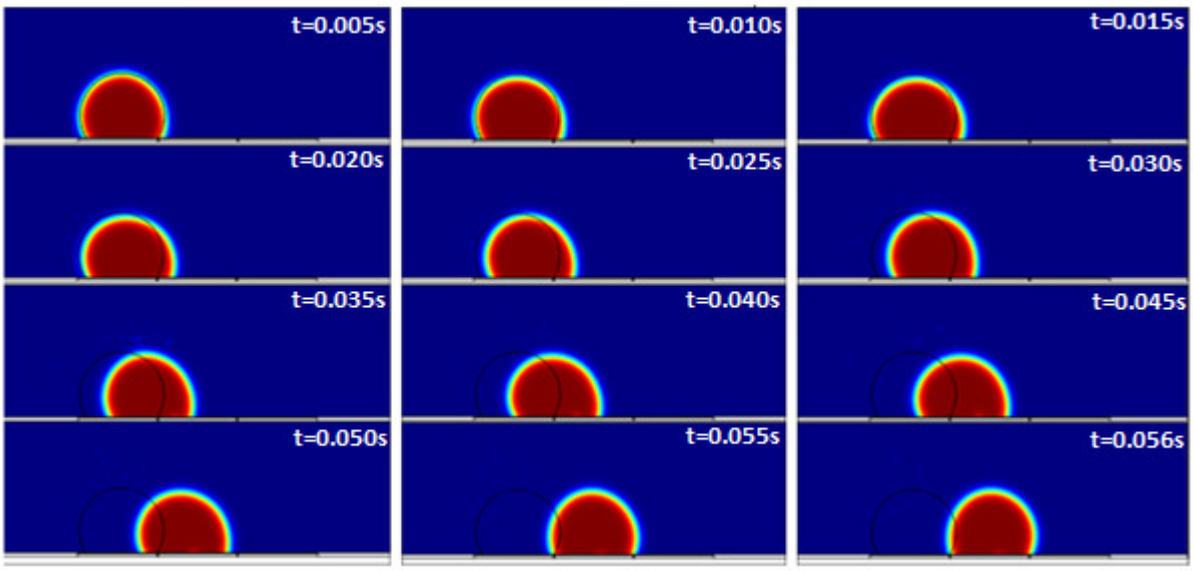

Figure 5.8: Transport of droplet to the adjacent electrode

5.1.5 Demonstrating dependency of velocity of droplet on voltage applied (Brochards model)

Brochards model states that velocity of moving droplet is proportional to applied voltage. To validate this model numerically, COMSOL analysis is performed using electrostatics and laminar two phase flow, level set method. Voltages chosen for this study are 16V, 20V, 24V 26V and 28V. The simulation is performed for 0.056s. The droplet completely shifts from one electrode to the other when voltage applied is 28V. In other cases, the droplet is unable to cover the one electrode distance. This indirectly links velocity of moving droplet to applied voltage. Droplet positions at different time at different voltages are shown in fig(5.9).

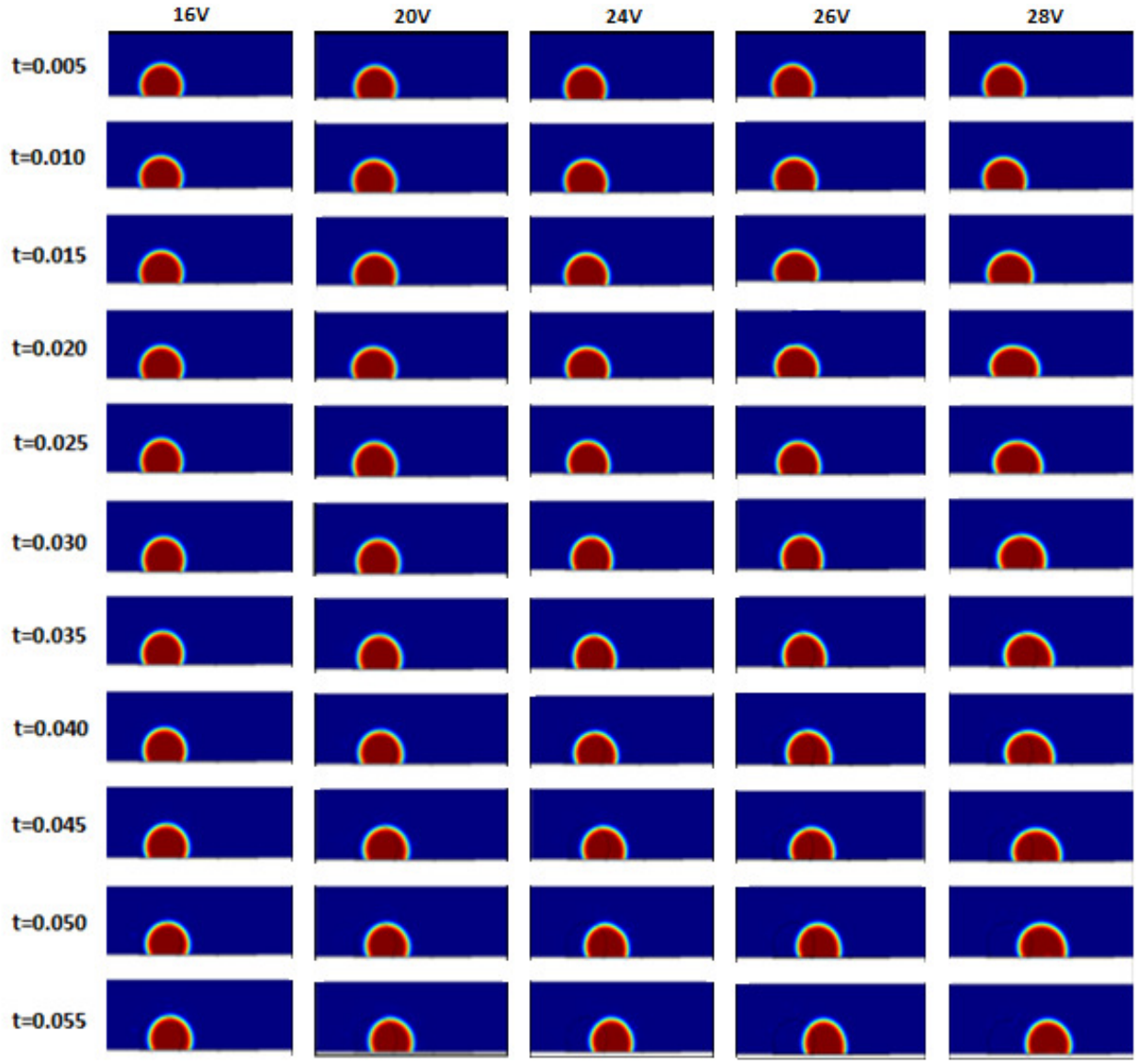

Figure 5.9: Droplet positions at different voltages

5.1.6 Realizing droplet transport over an array of electrodes

When droplet has to be moved over an array of electrodes, timings at which voltage is switched between the electrodes are important. To understand the optimum switching time, COMSOL simulation is performed. The fig (5.10) shows droplet position from 0s to 0.17s. Droplet moves over four electrodes in 0.1s. It takes more time to cross first electrode than the rest. The last electrode exerts electric force is opposite direction. This is the reason droplet oscillated around this electrode until it is stable.

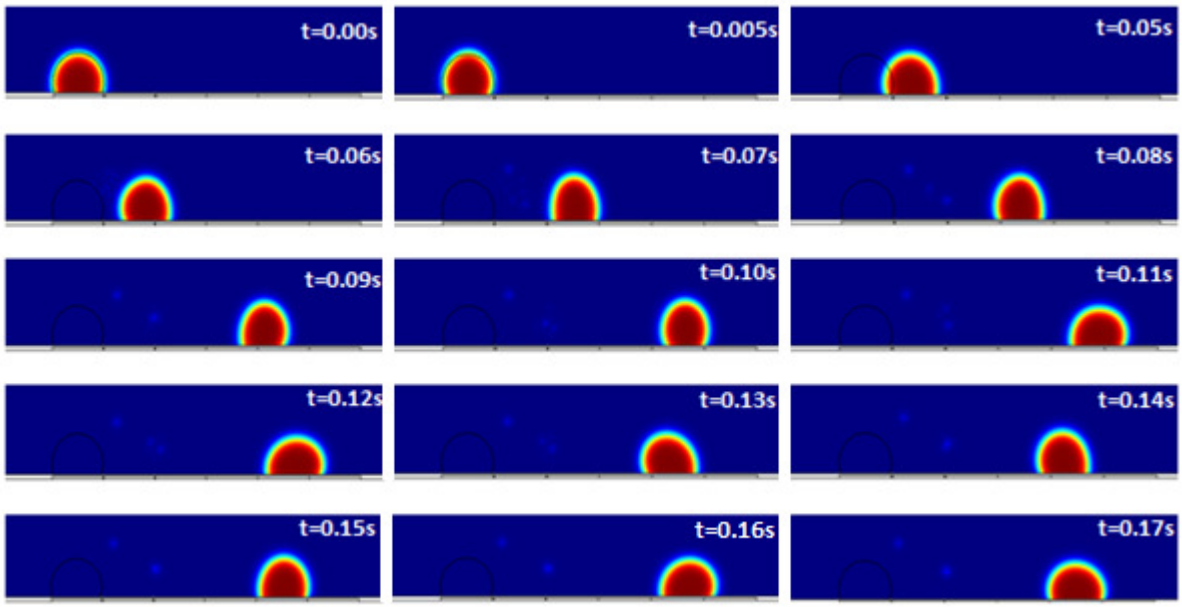

Figure 5.10: Transport of droplet over the array of electrodes

5.1.7 Demonstrating merging of two droplet

When EWOD devices are used in biological applications, multiple mixing and merging reactions are performed on chip. Either two droplets are merged at the centre electrode or one droplet is immobilized and the other droplet is allowed to freely move. To model this merging phenomenon, electrostatics and level set method are used. Two droplets are one electrode apart. The middle electrode is activated with 28V. Both the droplets move towards this activated electrode and merge. The interfaces of these droplets at different stages are shown in fig(5.11).

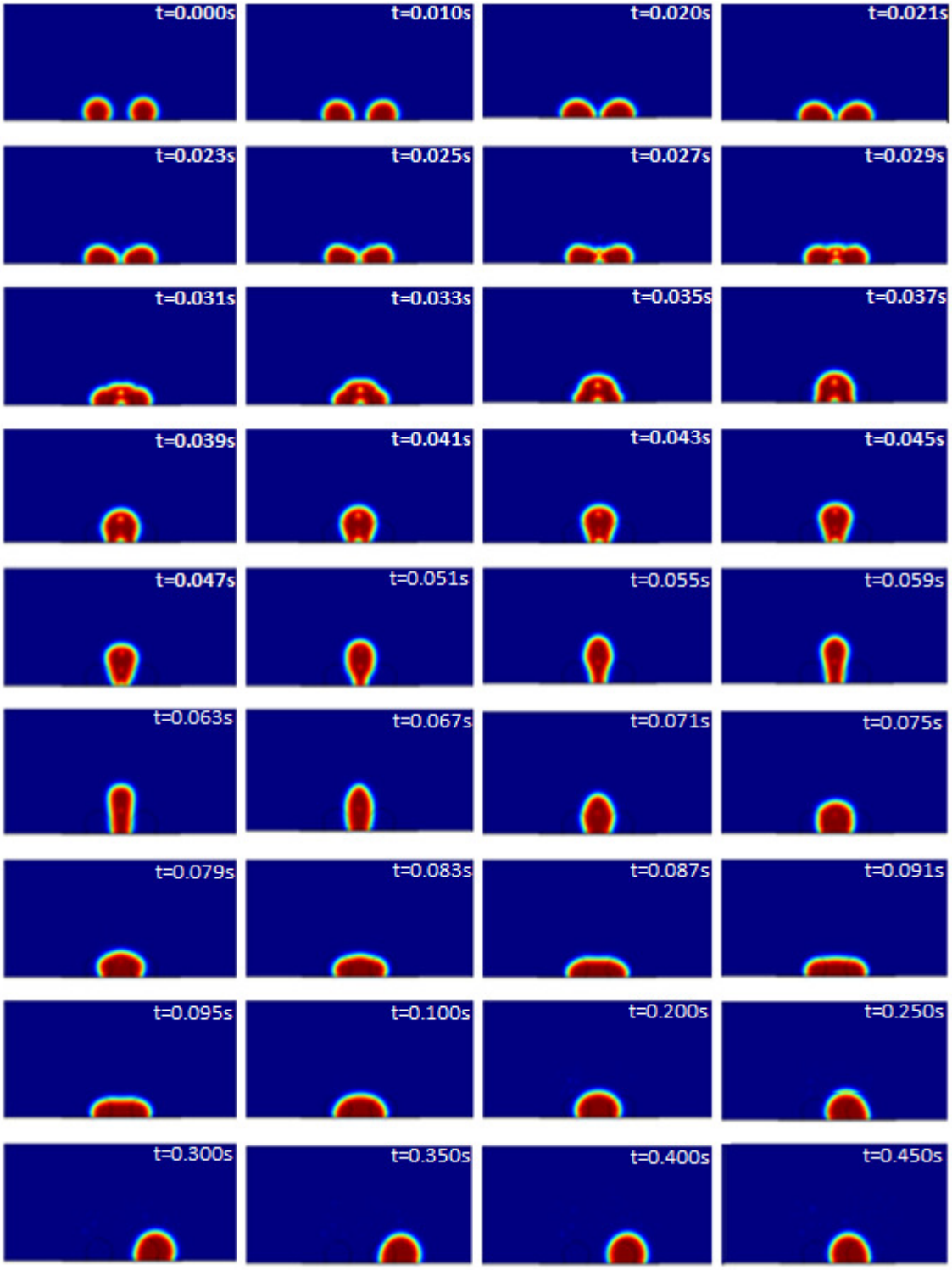

Figure 5.11: Merging of two droplets and transport of resultant droplet to the adjacent electrode

5.1.8 Visualizing concentration field after mixing

Merging of two droplets doesnt confirm uniform concentration of analytes in the resultant droplet. It is necessary to move the droplet over an array of electrodes.Due to computational time droplet has not been moved over the array of electrodes. When two droplets with concentration $1mol/m^3 and 0mol/m^3$ are mixed together, ideally, the resultant concentration should be $0.5mol/m^3$. This mixing of droplets occurs due to diffusion and vortices formed within the resultant droplet. This concentration field is visualized using transport of diluted species module in COMSOL.

The fig (5.12) demonstrates concentration field inside the droplet when applied with 28V.

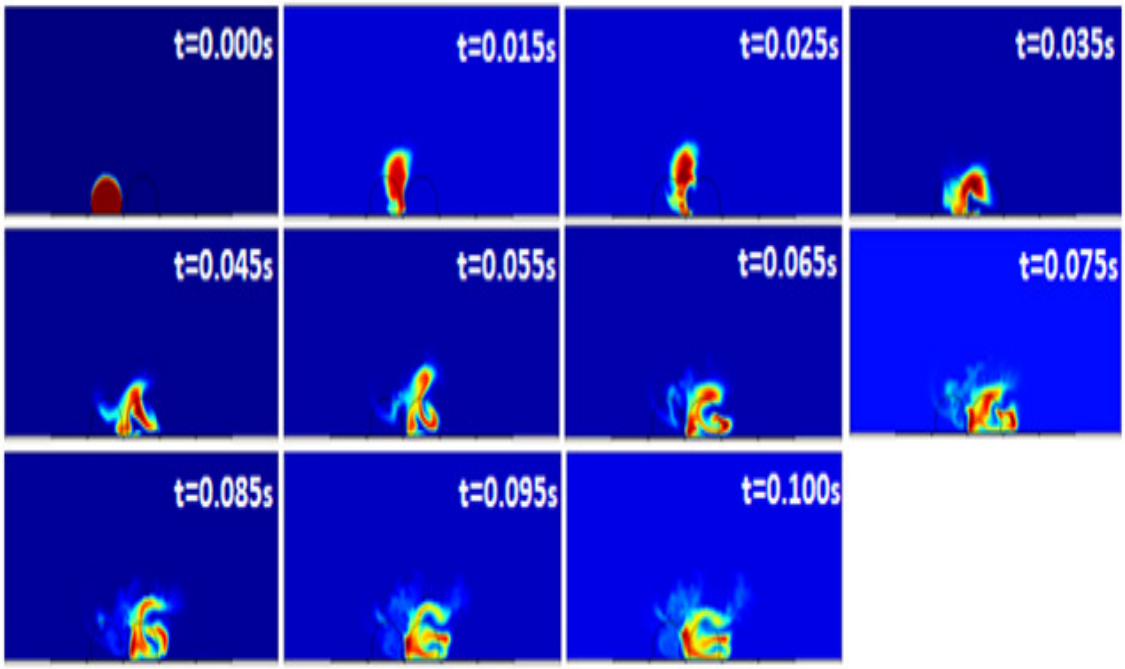

Figure 5.12: Concentration field studies at 28V

5.1.9 Demonstrating dependency of mixing quality on voltage applied

The quality of mixing is very important when biological applications are concerned. It is necessary to study the parameters that can change efficiency of mixing. One of the critical parameters that can change the quality of mixing is voltage level applied to electrodes.

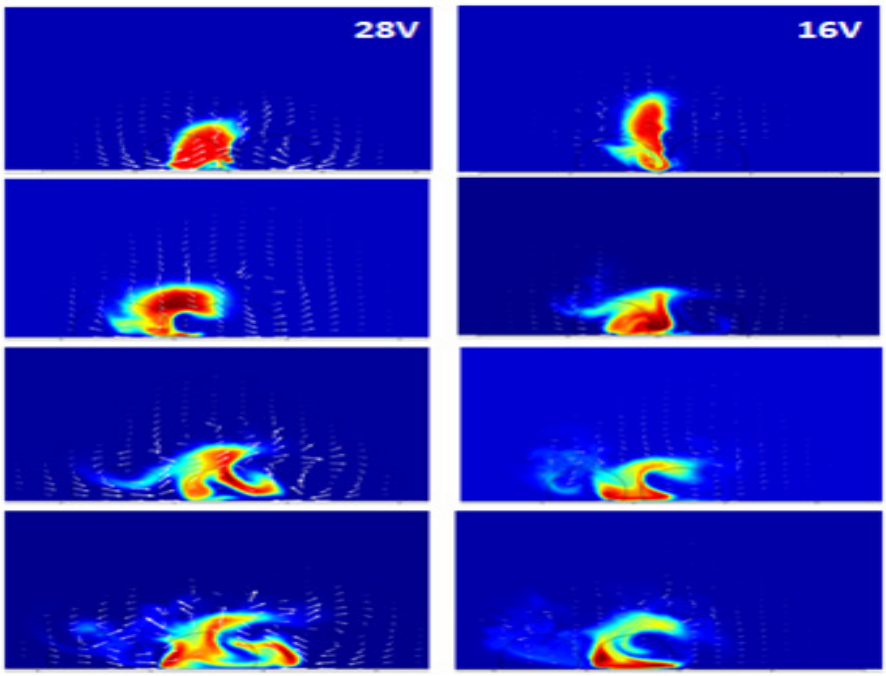

Figure 5.13: Velocity field studies at 28V and 16V

To verify this hypothesis, mixing of two water droplets with two different concentrations is performed with five different voltage levels applied to the electrode. These values are 16V, 20V, 24V, 26V and 28V. The simulation is performed for 0.1s. Values of concentration at different stages in one droplet are listed in table(5.3)

-	0.00s	0.01s	0.02s	0.03s	0.04s	0.05s	0.06s	0.07s	0.08s	0.09s	0.10s
28V	1	1	1	0.95	0.856	0.822	0.81	0.79	0.77	0.755	0.6
26V	1	1	1	0.99	0.973	0.957	0.94	0.92	0.90	0.88	0.83
24V	1	1	1	1	0.99	0.98	0.97	0.94	0.901	0.887	0.85
20V	1	1	1	1	0.991	0.98	0.976	0.97	0.96	0.92	0.89
16V	1	1	1	1	0.995	0.98	0.979	0.978	0.96	0.93	0.87

Table 5.3: Values of concentration in mol/m^3 at different time frames

These are the observations derived from numerical analysis. The next section in this chapter describes the experimental results.

5.2 Experimental Results

Indium Tin Oxide (ITO) electrodes are fabricated on glass substrate as discussed already. The fabricated EWOD device is then connected to electronic switching circuit. Droplets of KCl (15mS), PBS (5.8mS) and DI (0.1mS) water are placed over electrodes. These electrodes are activated with 5Vdc. The silicon nitride film is destroyed even at voltage as low as 5V. The calculated breakdown is 45V for 150nm. The bubbles are formed inside all liquid droplets indicating electrolysis of the liquid. This is observed in the EWOD devices with both the values of dielectric thickness. Fig 5.14 show these destroyed films.

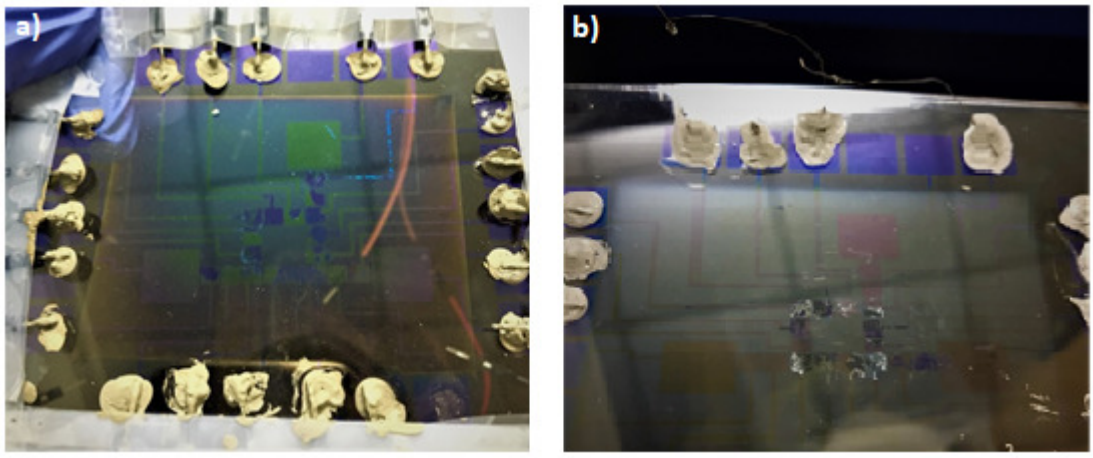

Figure 5.14: a)Destroyed silicon nitride film, d=70nm b)Destroyed silicon nitride film, d=150nm

To check the uniformity of silicon nitride film, these films are observed under the microscope. Multiple pinholes are observed in the silicon nitride films. These pinholes cause electrolysis of liquid droplets due to breakdown of dielectric film [28]. Fig5.15 shows these pinholes observed under microscope.

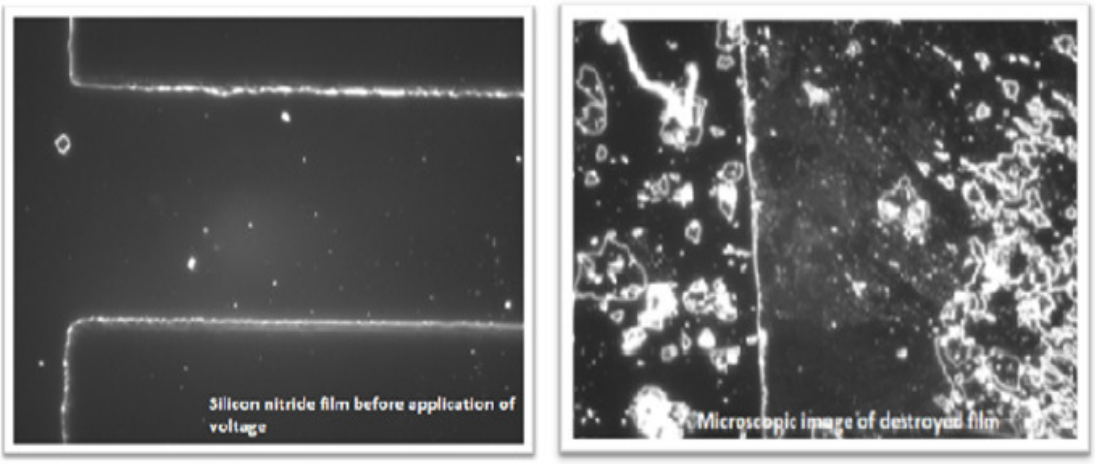

Figure 5.15: Pinhole in silicon nitride film before and after application of voltage

To avoid these pinholes, the EWOD chip is coated with Teflon AF solution. The Teflon has to be cured at 200 for 10 min. When the EWOD device is heated at 200, bubbles formed under the silicon nitride film. These bubbles are formed only in part where Teflon AF is dispensed which can be seen in fig(5.16). This confirms presence of pinholes in silicon nitride film.

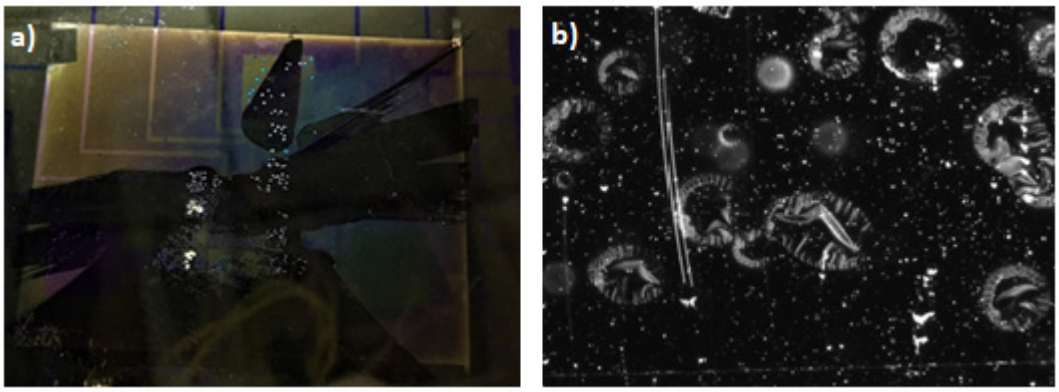

Figure 5.16: a)Bubbles formed under the Teflon coated silicon nitirde film b)Bubbles trapped under silicon nitride film can be seen in a microscopic picture

For finding the best suitable option as dielectric, SU8 and PDMS are coated on simple ITO coated glass substrate. SU8 is spin coated on ITO glass substrate at 3000rpm. This ITO glass was supplied by 5V. Electrolysis of liquid was observed which destroyed the film as well. Thus to increase the thickness of this SU8 film, two rounds of spin coating were done. This ITO glass was also supplied with 5V. But this film was also destroyed due to electrolysis of droplets of KCl, PBS and DI water which can be seen in fig(5.17).

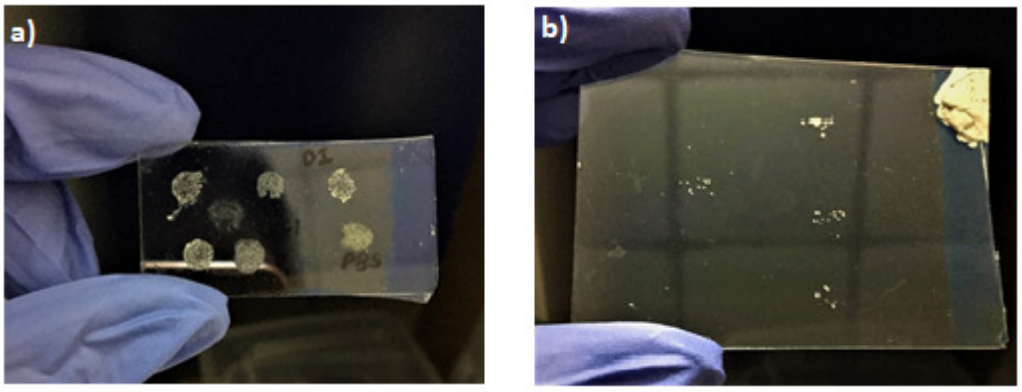

Figure 5.17: a)SU8 film destroyed after application of 5V b)Comparitively thicker SU8 film destroyed after applying 5V

The second option for dielectric layer is PDMS. PDMS is hydrophobic and has dielectric constant of 2. The PDMS is spin coated on ITO glass at 4000rpm. Thickness measured is 30m. The PDMS film is supplied with 5V. The film is stable. Even after gradually increasing the voltage till 40V, PDMS film is stable as seen in fig(5.18). But there is no change in contact angle. Theoretically the required voltage to change contact angle of droplet by 10 is 200V.This is very high voltage when biological applications are concerned. To achieve electrowetting effect at lower voltage, PDMS has to be spin coated at very high speed. This will help to achieve lower thickness of PDMS and ultimately lower activation voltage.

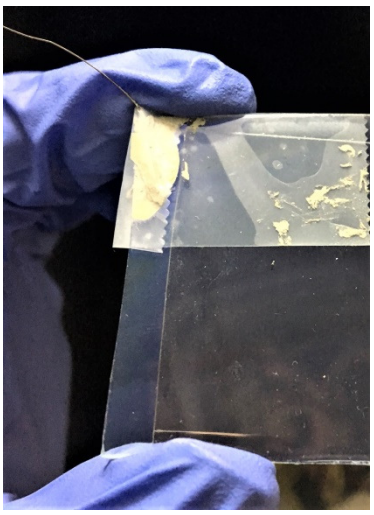

Figure 5.18: PDMS film after the application of 40V

5.3 Conclusion

This work presented the 2D simulations carried out to understand electrowetting effect, its dependency on voltage and dielectric thickness. It also discussed about 2D simulations for droplet transport over an electrode array, dependency of velocity of droplet and voltage, mixing of two droplets and dependency of mixing quality on applied voltage. The work also elaborately discussed about fabrication of EWOD device on Indium Tin Oxide (ITO) glass substrate. An electronic switching circuit is designed to control droplet motion on the fabricated EWOD device.

After the integration of EWOD device with electronic switching circuit, device is checked for contact angle change in droplets of KCl, PBS and DI water. Even with voltage as low as 5V, the dielectric film is destroyed. The main reason behind this observation is presence of pinholes in the nanofilm. Electrolysis of liquid droplet is caused due to these pinholes. The film is destroyed at voltage levels lower than the breakdown voltage of silicon nitride film.

In this work SU8 and PDMS are considered as alternatives for silicon nitride. The SU8 films, also, are destroyed causing electrolysis of the liquid droplets. In comparison to SU8, PDMS can withstand voltage levels up to 40V. To visualize contact angle change, this voltage is not sufficient. Thus reducing the thickness of PDMS film is very important.

To avoid pinholes in the silicon nitride, pressure enhanced chemical vapour deposition (PECVD) can be used. It can give better uniformity in silicon nitride nanofilms. Even changing the ITO substrate to substrate which forms passivating oxide layer can avoid electrolysis of the liquid droplet [18] Also to use PDMS as dielectric material, PDMS has to be spin coated at higher rpm. If we are able to achieve uniform dielectric film, this proposed EWOD device can be used as screening device for osteoporosis.

References

[1] Kim et al. “Micromachines driven by surface tension”. In: *American Institute of Aeronautics and Astronautics* (1999).

[2] Lee et al. “Electrowetting and electrowetting on dielectric for microscale liquid handling”. In: *Sensors and Actuators Physics: A* 95 (2002), pp. 259–268.

[3] Moon et al. “Low voltage electrowetting on dielectric”. In: *Journal of Applied Physics* 92 (2002), pp. 4080–4087.

[4] Pollack et al. “Electrowetting-based actuation of droplets for integrated microfluidics”. In: *Lab on a chip* 2 (2002), pp. 96–101.

[5] Cho et al. “Creating, transporting, cutting and merging liquid droplets by electrowetting- based actuation for digital microfluidic circuits”. In: *Journal of Microelectromechanical Systems* 12 (2003), pp. 70–80.

[6] Christopher G et al. “Electrowetting droplet microfluidics on a single planar surface”. In: *Microfluidics Nanofluidics* 2 (2006), pp. 435–446.

[7] Gupta et al. “A scheduling and routing algorithm for digital microfluidic ring layouts with bus-phase addressing”. In: *International conference on intelligent robots and systems* (2007).

[8] Whitesides. “The origins and futures of microfluidics”. In: *Nature* 442 (2007), pp. 368–373.

[9] Cahill et al. “A dynamic electrowetting simulation using level set method”. In: *COMSOL conference* (2008).

[10] Cho et al. “A high-performance droplet routing algorithm for digital microfluidic biochips”. In: *IEEE transactions on computer-aided-design of integrated circuits and systems* 27 (2008), pp. 1714–1724.

[11] Li et al. “Room-temperature fabrication of anodic tantalum pentoxide for low- voltage electrowetting on dielectric”. In: *Journal of Applied Physics* 17 (2008), pp. 1481–1488.

[12] Roland Baviere et al. “Dynamics of droplet transport induced by electrowetting actuation”. In: *Microfluidics Nanofluidics* 4 (2008), pp. 287–294.

[13] M Schneider. “An acoustically driven microliter flow chamber on a chip for cell cell and cell surface interaction studies”. In: *ChemPhysChem* 9 (2008), pp. 641–645.

[14] Brouzes E. “Droplet microfluidic technology for single-cell high-throughput screening”. In: *PNAS* 106 (2009), pp. 14195–14200.

[15] Qin G et al. “Biofunctionalization of alkylated silicon substrate surfaces via click chemistry”. In: *Journal of the American Chemical Society* 24 (2010), pp. 16432–16441.

[16] David A Weitz. “High-throughput injection with microfluidics using picoinjectors”. In: *PNAS* 107 (2010), pp. 19163–19166.

[17] Hao Gu et al. “Droplet formation and merging in two- phase flow microfluidics”. In: *Nature* 12 (2012), pp. 2572–2597.

[18] M Khodayari et al. “A material system for reliable low voltage anodic electrowetting”. In: *Materials letters* 69 (2012), pp. 96–99.

[19] Pogfai et al. “Design and experimental study of electrochemical detector with EWOD for chemical detection”. In: *Biomedical Engineering International Conference* (2012).

[20] Robert Barber. “Recent Advances in Electrowetting Microdroplet Technologies”. In: *Microdroplet technology: Principles and emerging applications in biology and chemistry* (2012), pp. 77–116.

[21] Aaron R Wheeler. “Digital Microfluidics”. In: *Annual review of Analytical Chemistry* 5 (2012), pp. 413–440.

[22] Dongen et al. “Simulation of the coalescence and subsequent mixing of inkjet printed droplets”. In: *COMSOL conference* (2013).

[23] D Caputo et al. “Polydimethylsiloxane material as hydrophobic and insulating layer in electrowetting on dielectric systems”. In: *Microelectronics Journal* 45 (2014), pp. 1684–1690.

[24] Tsung Yi Ho et al. “Chip level design for digital microfluidic biochips”. In: *Microfluidics Nanofluidics* 4 (2014), pp. 202–207.

[25] Xiong et al. “Design and simulation of high throughput microfluidic droplet dispenser of lab on a chip applications”. In: *COMSOL conference* (2014).

[26] Yu et al. “Chip-level design for digital microfluidic biochips”. In: *International Journal of Automation and Smart Technology* 4 (2014), pp. 202–207.

[27] Anuradha Khadilkar et al. “Epidemiology and treatment of osteoporosis in women: an Indian perspective”. In: *International Journal on Women’s health* 7 (2015), pp. 841–850.

[28] Da Jeng Yao et al. “Improving the dielectric properties of an electrowetting-on-dielectric microfluidic device with a low-pressure chemical vapor deposited Si3N4 dielectric layer”. In: *Biomicrofluidics* 9 (2015).

[29] Nahar et al. “Numerical modelling of 3D electrowetting droplet actuation and cooling of a hotspot”. In: *COMSOL conference* (2015).

[30] Najjaran et al. “Ultra-portable smartphone controlled integrated digital microfluidic system in 3D-printed modular assembly”. In: *Micromachines* 6 (2015), pp. 1289–1305.

[31] Pop et al. “Synthesis of biochemical applications on digital microfluidic biochips with operation execution time variability”. In: *INTEGRATION, the VLSI journal* (2015), pp. 158–168.

[32] Vetterling et al. “Multiphase laminar flow with more than two phases”. In: *COMSOL conference* (2015).

[33] Martino C et al. “Droplet-based microfluidics for artificial cell generation, a brief review”. In: *Interface focus* (2016).

[34] JI Xing Hu. “Colorimetric detection of alkaline phosphatase on microfluidic paper- based analysis device”. In: *Chinese Journal of Analytical Chemistry* 44 (2016), pp. 591–596.

[35] Elias Yazdanshenas. “Electrowetting Using a Microfluidic Kelvin Water Dropper”. In: *Micromachines* 9 (2018).